ON REYNOLDS STRESSES AND TURBULENT FLOWS IN CIRCULAR DUCTS

A THESIS

Presented to

The Faculty of the Division of Graduate

Studies and Research

By

Kenneth Alan Williams

In Partial Fulfillment

of the Requirements for the Degree

Master of Science in Mechanical Engineering

Georgia Institute of Technology

June, 1974

ON REYNOLDS STRESSES AND TURBULENT FLOWS

IN CIRCULAR DUCTS

Approved:

Novak Zuber, Chairman

Ward O. Winer

P. V. Desai

Charles W. Gorton

Date approved by Chairman: May 17, 1974

ACKNOWLEDGMENTS

The author wishes to express his deep appreciation to his advisor, Dr. Novak Zuber, for suggesting the thesis area and for his devoted assistance which made the success of this work possible. The author is also grateful for the valuable career guidance given him by his advisor.

It is a pleasure to thank Drs. Winer and Desai of the School of Mechanical Engineering and Dr. Gorton of the School of Chemical Engineering, for their interest in the work and for their meaningful comments and suggestions.

Finally the author wishes to express his gratitude toward his entire family, whose continued encouragement and support made his education possible.

TABLE OF CONTENTS

LIST OF ILLUSTRATIONS

NOMENCLATURE

a	a constant in van Driest equation
b	a constant in the model
c()	indicates functional dependency on ()
c_4, c_5	constants defined by equation (III-2)
D	pipe diameter
E()	indicates functional dependency on ()
f	Moody friction factor
F()	indicates functional dependency on ()
f()	indicates functional dependency on ()
G()	indicates functional dependency on ()
k	von Karman "universal constant" equal to 0.4
L	unit length
m	exponent of Reynolds number in power approximation
n	nondimensional distance from the pipe wall based on radius
N	a constant in the model
p	absolute pressure
Δp	pressure drop
Re	Reynolds number based on pipe diameter and average velocity
R_*	Reynolds number based on friction velocity and pipe radius
r	radius variable
r_w	pipe radius

t_o	reference time
T	time
τ_T	total shear stress
τ_L	shear stress due to viscous forces (laminar effects)
τ_R	Reynolds stress
τ_w	wall shear stress
v	velocity
v_*	friction velocity
v^+	nondimensional velocity
v_i'	fluctuating component of velocity
$\overline{v_i}$	time averaged value of the velocity
$w()$	indicates functional dependency on ()
y	distance from the pipe wall
y^+	nondimensional distance from the pipe wall based on wall shear stress and viscosity
z	axial coordinate in the pipe
ℓ	mixing length
ℓ^+	nondimensional mixing length
μ	fluid viscosity
μ_T	turbulent viscosity
ν	fluid kinematic viscosity
ν_T	turbulent kinematic viscosity (eddy diffusivity)
ν_e	"effective" viscosity
ρ	fluid density
ℓn	natural logarithm
$\tan^{-1}()$	arctangent ()

SUMMARY

A position dependent model of the Reynolds stresses is proposed. The model is offered as an alternative to the presently accepted "gradient-transport models." The model is shown to satisfy the constraints that must be placed upon any model of turbulence, that is, the model satisfies the physical boundary conditions of pipe flow, basic analytical formulations and experimental data.

The Reynolds stress model is shown to be in agreement with experimental data very near the pipe wall, as well as in the core region. The velocity distribution is obtained by integration of the Reynolds equation with the present analysis used to model the Reynolds stresses. The resulting expression for the velocity distribution is shown to be in agreement with experimental data throughout the pipe, that is, from the wall to the pipe centerline. The "velocity defect law" is determined in terms of the present analysis and compared against experimental data. The friction factor based on the present analysis is given as a function of Reynolds number and is compared with the "Moody chart" as well as with experimental data. An eddy diffusivity model is presented in terms of the present analysis and is compared with experimental data near the wall and in the core. Finally, a review of the presently employed models of turbulence is given.

CHAPTER I

INTRODUCTION

1.1 Significance of the Problem

To develop an accurate model of turbulent flows is one of the challenging problems confronting fluid dynamicists. Although the problem has received considerable attention in the past, it is still of great importance because of the development of modern nuclear, petroleum and chemical systems. The maximazation of plant efficiency and the safety analysis of nuclear reactors relies heavily upon our understanding of turbulent flows. This is a consequence of the coupling between fluid flow and the transport of energy in convective heat transfer. The petroleum industry must presently transport their products through pipelines over long distances, there emphasizing the economics of a detailed understanding of the frictional losses in turbulent flows. Enhancement of mass transport that is associated with turbulent flows is important in the optimization of chemical systems. Thus, if the technology is to continue to progress at the present rate, then the designers of modern systems must be furnished with an accurate model of turbulence.

1.2 Purpose of the Thesis

The purpose of the thesis is to propose a new approach

at modeling Reynolds stresses and turbulent flows; the model being applicable to steady, nonisotropic turbulent flows in circular ducts.

In particular, it is the objective of this thesis to present a model (based on Reynolds stresses) which can be used to predict (a) the velocity profile throughout the pipe, that is from the wall to the pipe center; (b) the average velocity; (c) the friction factor and thus the pressure losses and (d) the eddy diffusivity throughout the pipe.

CHAPTER II

BASIC FORMULATION AND DISCUSSION

2.1 Analytical Formulation of Basic Relationships

2.1.1 Shear Stress Distribution

In general, we can make a force balance on a fluid cylinder in steady pipe flow; the results must be valid for all flow regimes, that is, for both turbulent and laminar flows,

$$\text{Pressure Forces} = \text{Shear Forces} \tag{II-1}$$

$$\Delta P \pi r^2 = \tau(r) 2\pi r L \tag{II-2}$$

Rearranging,

$$\tau(r) = \frac{\Delta P}{L} \frac{r}{2} \tag{II-3}$$

Thus

$$\tau(r_w) \equiv \tau_w = \frac{\Delta P}{L} \frac{r_w}{2} \tag{II-4}$$

Nondimensionalizing the shear,

$$\frac{\tau(r)}{\tau_w} = \frac{r}{r_w} = (1-n) \qquad \text{(II-5a)}$$

where

$$n \equiv y/r_w = 1 - \frac{r}{r_w} \qquad \text{(II-5b)}$$

(the relative distance from the wall)

From (5) it is apparent that the total shear stress in steady pipe flow is a linear function of the relative distance from the pipe center for turbulent as well as for laminar flow (see Figure 1).

2.1.2 Reynolds Equation

The Navier-Stokes equations are of course applicable to turbulent flow. The difficulty in applying these equations to turbulent flow lies in the fact that the variables in the equations refer to the instantaneous values at the point under consideration. These values vary to such a degree that little information can be gained by direct application of the basic theory, and thus some form of modification or extension is required. An approach was introduced by Osborne Reynolds in 1895 that greatly simplified these equations. Reynolds decomposed the turbulent variables into a mean value plus a fluctuation, with the time averaged value of the fluctuation equal zero. That is,

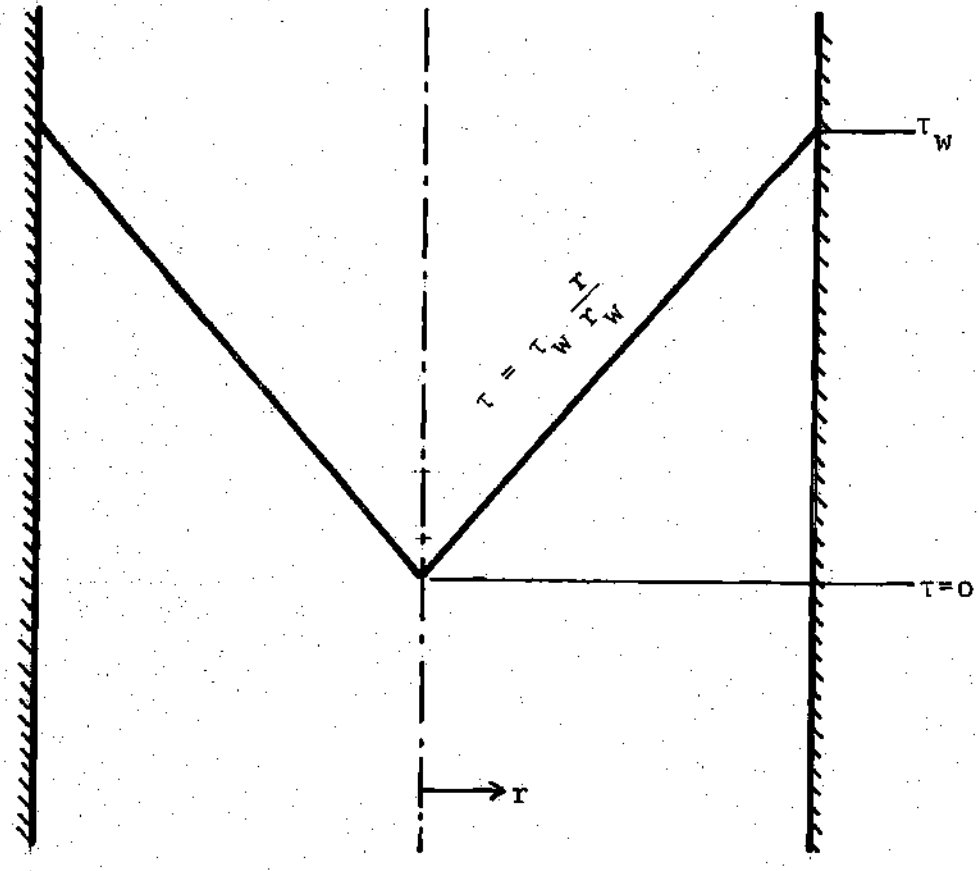

Figure 1. Total Shear Stress Distribution

$$v_i \equiv \bar{v}_i + v_i' \tag{II-6}$$

where

$$\bar{v}_i = \text{mean value of the } i^{th} \text{ component of the variable } v \tag{II-7}$$

$$v_i' = \text{fluctuation of the } i^{th} \text{ component of the variable } v \tag{II-8}$$

$$\bar{v}' = \lim_{T\to\infty} \frac{1}{T} \int_{to}^{to+T} (v_i - \bar{v}_i)dt = 0 \tag{II-9}$$

In general, it is true that

$$\overline{v_i' v_j'} \neq 0 \tag{II-10}$$

if the flow is turbulent.

By substituting the decomposed velocity into the Navier-Stokes equation, Osborne Reynolds arrived at the time averaged momentum equation applicable to turbulent flows. In his honor, this momentum equation is termed the Reynolds equation. The Reynolds equation is derived in Appendix A and the result is given here in cylindrical coordinates for steady flow.

$$\frac{\partial P}{\partial z} = -\frac{1}{r}\frac{\partial}{\partial r}\left[r\left(-\mu\frac{\partial v}{\partial r}\right)\right]-\frac{1}{r}\frac{\partial}{\partial r}\left[r\left(\rho\overline{v_r' v_z'}\right)\right] \qquad \text{(II-11)}$$

It is noted that the Reynolds equation is identical with the laminar flow momentum equation, except for the last term,

$$\rho\ \overline{v_r' v_z'} = \tau_R \qquad \text{(II-12)}$$

where τ_R is termed the Reynolds stress. The Reynolds equation can be expressed as

$$\frac{\partial P}{\partial z} = -\frac{1}{r}\frac{\partial}{\partial r} r[\tau_L + \tau_R] \qquad \text{(II-13)}$$

For steady state, fully developed flow it is assumed that the pressure gradient is constant, i.e.

$$\frac{\partial P}{\partial z} = -\frac{\Delta P}{L} \qquad \text{(II-14)}$$

Thus, integration of equation (13) gives

$$\frac{\Delta P}{L}\frac{r}{2} = \tau_L + \tau_R \qquad \text{(II-15)}$$

Employing equation (3),

$$\tau = \tau_L + \tau_R \qquad \text{(II-16)}$$

where τ is the total shear stress already shown to be a linear function of r. By definition equation (16) becomes

$$\tau = -\mu \frac{dv}{dr} + \rho \overline{v_r' v_z'} \qquad \text{(II-17)}$$

Employing equation (5a)

$$\tau_w(1-n) = -\mu' \frac{dv}{dr} + \rho \overline{v_r' v_z'} \qquad \text{(II-18)}$$

Defining

$$v_*^2 = \tau_w/\rho \qquad \text{(II-19)}$$

where v_* is the "friction velocity" equation (18) becomes

$$(1-n) = -\frac{\nu}{v_*^2} \frac{dv}{dr} + \frac{\overline{v_r' v_z'}}{v_*^2} \qquad \text{(II-20)}$$

Notice that the Reynolds stress terms can be expressed as,

$$\frac{\overline{v_r' v_z'}}{v_*^2} = \frac{\rho \overline{v_r' v_z'}}{\tau_w} = \frac{\tau_R}{\tau_w} \qquad \text{(II-21)}$$

and thus it scales the turbulent stress with the wall stress. Equation (20) can be expressed in dimensionless form by defining a

$$\text{Nondimensional velocity; } v^+ = \frac{v}{v_*} \qquad \text{(II-22)}$$

and a

$$\text{Nondimensional length; } y^+ = \frac{yv_*}{\nu} \qquad \text{(II-23)}$$

Substituting equation (22) and (23) into equation (20) yields

$$(1-n) = \frac{dv^+}{dy^+} + \frac{\overline{v'_r v'_z}}{v_*^2} \qquad \text{(II-24)}$$

Defining a Reynolds number based on frictional velocity,

$$R_* = \frac{v_* r_w}{\nu} \qquad \text{(II-25)}$$

Thus in view of equation (5b)

$$n = y/r_w = y^+/R_* \qquad \text{(II-26)}$$

From equation (26) note that as n varies between 0 and 1, y^+ varies between 0 and R_*, and that R_* itself may vary from approximately 70 for laminar flow to 10,000 or larger for very turbulent flow. Thus equation (24) becomes,

$$(1-n) = \frac{1}{R_*}\frac{dv^+}{dn} + \frac{\overline{v'_r v'_z}}{v_*^2} \qquad \text{(II-27)}$$

Equation (24) and (27) are the differential equations of motion that will be used extensively in the present analysis.

2.1.3 Closure Problem

An examination of the Reynolds equation reveals that the equation contains two dependent variables: the velocity and the Reynolds stress. Having two unknowns and only one equation results in a closure problem. In order to obtain a unique solution to the differential equation, the dependence of one of the dependent variables on the independent variable must be assumed. Mathematically the choice is arbitrary; from a practical standpoint it is desirable to obtain the velocity distribution, thus, it is necessary to assume an expression for the turbulent stress and solve the differential equation to yield the velocity as a function of position.

2.2 Present Methods

There are presently several methods employed to specify the Reynolds stress, the most significant being the mixing length hypothesis due to L. Prandtl [1] and the eddy diffusivity model due to Boussinesq [2]. Some of the present methods are reviewed in Appendix B.

The formulation of Prandtl assumes the turbulent stress to be proportional to a mixing length squared times the local velocity gradient squared, i.e.

$$\tau_R = \rho \ell^2 \left(\frac{d\bar{v}}{dy}\right)^2 \qquad \text{(II-28)}$$

An equation specifying the mixing length is required to obtain closure. The mixing length approach of Prandtl leads to a logarithmic velocity profile which is in satisfactory agreement with the experimental data. However, after an analysis of the mixing length approach, Tennekes and Lumley [3], state that "a gradient-transport model which links stress to the rate of strain at the same point in space and time cannot be used for turbulent flow."

The concept of eddy diffusivity assumes the turbulent stress to be proportional to an eddy viscosity times the local velocity gradient, i.e.

$$\tau_R = \mu_T \frac{d\bar{v}}{dy} \qquad \text{(II-29)}$$

In order to obtain closure an equation specifying the eddy viscosity as a function of position is required. The eddy diffusivity concept is also very important in the analysis of the turbulent transport of thermal energy.

2.3 General Observations Concerning Turbulent Flow

Turbulent flow may be analyzed by dividing the flow into two regions, each having different characteristics that govern the flow. This introduces the so-called "problem of multiple length scales" and is a criterion that distinguishes laminar flow, which has a single length scale (the diameter), from the turbulent flow regime. These two hydrodynamic regions are termed the inner region and the outer region,

with the inner region characterizing flow near a bounding surface and the outer region characterizing flow in the core. The flow near a wall is governed by both viscosity and the local distance from the wall itself; it is not influenced by the wall curvature thus being independent of the pipe diameter. Prandtl proposed that it is within this narrow region that turbulent energy is dissipated by viscosity. In the inner region the characteristic length is $\frac{\nu}{\sqrt{\frac{\tau_w}{\rho}}}$, scaling the local distance from the wall gives

$$y^+ = \frac{y\sqrt{\tau_w/\rho}}{\nu} \qquad \text{(II-30)}$$

the quantity $\sqrt{\frac{\tau_w}{\rho}}$ is often termed the "friction velocity" since it has the units of velocity and it is used to scale the turbulent velocity. Thus, near the wall

$$\frac{v}{v_*} = f(y^+) \qquad \text{(II-31)}$$

This is the "law of the wall," first suggested by Prandtl.

In the core (or in the wake for a flat plate) viscosity plays little role in determining the flow pattern; it should be noted however, that just how far from the wall this is true is determined by y^+ which itself accounts for the fluid viscosity. In the core the characteristic length is the pipe diameter and it becomes necessary to define a second nondimensional length n,

$$n \equiv y/r_w \qquad \text{(II-32)}$$

Thus in the core,

$$\frac{v}{v_*} = g(n) \qquad \text{(II-33)}$$

and the velocity profile is independent of fluid viscosity, i.e. there exists what von Karman termed "Reynolds number similarity." This is in fact the case only for large Reynolds numbers, where by definition the inertial forces are large compared to the viscous forces. If the difference between the maximum velocity and the velocity at any point in the core is rendered dimensionless with the friction velocity, this velocity difference is a function of the relative distance from the wall alone; this is the so-called "velocity defect law" due to von Karman and characterizes flow far from a bounding surface, i.e.

$$\frac{v(1)-v(n)}{v_*} = G(n) \qquad \text{(II-34)}$$

2.4 Comments and Conclusions

The turbulence models that are presently being employed by fluid dynamicists give fair agreement with experimental data in certain regions of the pipe. However, these models are known to be deficient in the proximity of the wall or

the pipe center, or in both regions. The "state of the art" consists of piecing together three velocity expressions in order to obtain the velocity from the wall to the pipe center:

$$v^+ = y^+ \qquad 0 \leq y^+ < 5 \qquad \text{(II-35a)}$$

$$v^+ = 5.0 \ln y^+ - 3.05 \qquad 5 < y^+ < 30 \qquad \text{(II-35b)}$$

$$v^+ = 2.5 \ln y^+ + 5.5 \qquad y^+ > 30 \qquad \text{(II-35c)}$$

The mixing length approach results in a logarithmic velocity distribution; it is easily verified that the "log law" is indeterminate at the wall and results in a nonzero shear stress at the pipe centerline. Furthermore, an equation describing the mixing length is required for closure. The mixing length is difficult to obtain experimentally since the velocity gradient must first be determined and with the flat profile in turbulent flow it is difficult to accurately measure the gradient. Moreover, it is shown in Appendix B that the mixing length becomes indeterminate at the pipe centerline.

The eddy diffusivity approach suffers from the lack of a general formulation predicting the turbulent viscosity as a function of the relative distance from the wall. It is pointed out by Kays [29] that the eddy diffusivity model employed in convective heat transfer has a discontinuity at

$y^+ = 30$ and predicts negative values of $\frac{\nu_T}{\nu}$ near the pipe center. In Appendix B, Diessler's [12] and van Driest's [25] approach is shown to be incorrect in approaching the wall. Thus, the eddy diffusivity concept is still lacking a unified model of the turbulent viscosity.

Both of these turbulent models, the mixing length hypothesis and the eddy diffusivity, formulate a relationship between the turbulent stress and the local velocity gradient. This approach is shown to be incorrect by Tennekes and Lumley [3], as mentioned in Section 2.2. However, due to the current information (both experimental and analytical) concerning Reynolds stresses in circular ducts, it is possible to formulate the Reynolds stresses as a function of position alone. This is the approach taken in this thesis.

CHAPTER III

PRESENT ANALYSIS

3.1 Outline of the Present Analysis

The approach taken in the present analysis to model steady, nonisotropic turbulent flow in circular ducts can be summarized as follows. First, the Reynolds stress will be postulated as a function of position. Evidence is given to demonstrate that this model satisfies both analytical and experimental requirements on Reynolds stresses. With the Reynolds stress postulated as a function of position, the Reynolds equation (II-24) or (II-27) is integrated to yield the velocity distribution as a single, continuous function from the wall to the pipe centerline. The proposed model requires a zero velocity at the wall and a zero velocity gradient at the centerline. Integrating this velocity distribution over the pipe crossection yields the average velocity. The friction factor is immediately obtained from the nondimensional average velocity. Finally, the present analysis is employed to determine the eddy diffusivity throughout the entire pipe.

3.2 Reynolds Stresses

There are presently numerous accounts of experimental measurements in turbulent velocity fluctuations. The two

most notable of these being due to Laufer [4] and Sandborn [5] both of whom experimentally measured the root mean square velocity fluctuation as a function of position in fully developed pipe flow. These accounts conclude that in the pipe core the total stress is due almost entirely to turbulent fluctuation, with viscous forces playing little role. Thus, in the core the Reynolds stress must decrease to zero at the centerline as does the total stress (see Section 2.1.1). Both Laufer and Sandborn used hot wire anemometers to measure the velocity fluctuations and thus had some uncertainty in the near wall measurements. The velocity fluctuation near the wall can also be measured with a laser doppler technique so as not to disrupt the flow. Thus, there are sufficient experimental results presently available to check the validity of a position dependent model of Reynolds stresses.

Analytical formulations of the velocity profile very near the wall have been presented in the literature. The first formulation was apparently given by Murphree [6]. It has been analytically shown by Hinze [7], Townsend [8], and Monin and Yaglom [9] that the velocity must approach the wall as a polynominal containing y^+ to the first, fourth, and fifth powers. That is,

$$\lim_{y^+ \to o} v^+ = y^+ - c_4 y^{+4} + c_5 y^{+5} \qquad \text{(III-1)}$$

This result is obtained by differentiating equation (II-17) with respect to y^+ and expressing the mean velocity by Taylor series expansion at $y^+=o$. This procedure yields the constants c_4 and c_5,

$$c_4 = \frac{-\nu^3}{24v_*^5}\left(\frac{\partial^3\overline{v_r'v_z'}}{\partial y^{+3}}\right)\Big|_{y^+=o} \qquad \text{(III-2a)}$$

$$c_5 = \frac{\nu^4}{120v_*^6}\left(\frac{\partial^4\overline{v_r'v_z'}}{\partial y^{+4}}\right)\Big|_{y^+=o} \qquad \text{(III-2b)}$$

Note that due to the closure problem, $\overline{v_r'v_z'}$ (and thus c_4 and c_5) cannot be determined without first knowing the velocity distribution. Tien and Wasan [10] used experimental data to determine these constants and suggest the following equation to represent the velocity profile very near the wall,

$$v^+ = y^+ - 7.8 \times 10^{-5}y^{+4} + 2.1 \times 10^{-6}y^{+5} \qquad \text{(III-3)}$$

This equation is in agreement with experimental data from the wall to $y^+ \approx 20$. Substituting equation (III-1) into the Reynolds equation yields the form in which the Reynolds stress must approach the wall,

$$\lim_{y^+\to o} \frac{\overline{v_r'v_z'}}{v_*^2} = 4c_4y^{+3} - 5c_5y^{+4} \qquad \text{(III-4)}$$

Thus, there are analytical formulations available that suggest the position dependency of the Reynolds stresses very near the wall as well as in the core and experimental data that can be used to evaluate a model.

3.3 Constraints on the Model

In order to satisfy the requirements of (i) boundary conditions in pipe flow, (ii) basic analytical formulations, and (iii) experimental data, the model must satisfy the following constraints:

(a) at $y^+ = o$

$$v^+ = o \tag{III-5}$$

$$\tau_R{}^+ \equiv \frac{\tau_R}{\tau_w} = o \tag{III-6}$$

$$\frac{\nu_T}{\nu} = o \tag{III-7}$$

(b) as $y^+ \to o$, that is, close to the wall

$$\lim_{y^+ \to o} v^+ = y^+ - c_4 y^{+4} + c_5 y^{+5} \tag{III-8}$$

This is needed to satisfy the results of [9]. Therefore,

$$\lim_{y^+ \to o} \frac{dv^+}{dy^+} = 1 - 4c_4 y^{+3} + 5c_5 y^{+4} \tag{III-9}$$

$$\lim_{y^+ \to o} \frac{\nu_T}{\nu} = 4c_4 y^{+3} - 5c_5 y^{+4} \qquad \text{(III-10)}$$

$$\lim_{y^+ \to o} \tau_R^+ = 4c_4 y^{+3} - 5c_5 y^{+4} \qquad \text{(III-11)}$$

(c) as y^+ increases,

τ_R^+ goes through a maximum at n_e (or y_e^+)

therefore at n_e,

$$\frac{d\tau_R^+}{dn} = o \qquad \text{(III-12)}$$

$$\frac{d^2\tau_R^+}{dn^2} < o \qquad \text{(III-13)}$$

(d) in the intermediate region, that is, when

$$y^+ >> 1 \text{ but } n = \frac{y^+}{R_*} << 1$$

we have the "law of the wall,"

$$v^+(y^+) = \frac{1}{k} \ln (y^+) + \text{constant} \qquad \text{(III-14)}$$

this is the constant stress region where,

$$\tau_R^+ \approx \text{constant} \qquad \text{(III-15)}$$

and

$$\frac{\nu_T}{v_* r_w} \approx kn \qquad \text{(III-16)}$$

(e) in the core, that is, when

$$n = \frac{y^+}{R_*} \to 1$$

the "velocity defect law" is applicable,

$$v^+(1) - v^+(n) = \frac{1}{k} G(n) \qquad \text{(III-17)}$$

and

$$v^+(y^+) = \underbrace{\frac{1}{k} \ell n\ (y^+) + \text{constant}}_{\text{"law of the wall"}} + \underbrace{\frac{1}{k} w(n)}_{\text{"law of the wake"}} \qquad \text{(III-18)}$$

and

$$\tau_R^+ \text{ decreases to zero} \qquad \text{(III-19)}$$

(f) at the pipe center, that is, when n = 1,

$$v^+ = v^+_{max} \qquad \text{(III-20)}$$

therefore

$$\frac{dv^+}{dn} = o \qquad \text{(III-21a)}$$

$$\frac{d^2v^+}{dn^2} < o \qquad \text{(III-21b)}$$

Also,

$$\tau^+_R = o \qquad \text{(III-22)}$$

$$\frac{\nu_T}{v_* r_w} = \text{finite} \qquad \text{(III-23)}$$

3.4 The Model

In what follows, it will be shown that the proposed model satisfies all the requirements listed in the previous section. Recall the Reynolds equation,

$$\frac{dv^+}{dy^+} = (1-n) - \frac{\overline{v'_r v'_z}}{v_*^2} \qquad \text{(III-24)}$$

We shall express the dimensionless Reynolds stress by

$$\tau_R^+ = \frac{\overline{v_r' v_z'}}{v_*^2} \equiv F(n) \equiv f(y^+)(1-n) \qquad \text{(III-25)}$$

Substituting (25) into (24),

$$\frac{dv^+}{dy^+} = \{1-f(y^+)\}\ (1-y^+/R_*) \qquad \text{(III-26)}$$

when $y^+/R_* << 1$ this reduces to

$$\frac{dv^+}{dy^+} \approx 1-f(y^+) \qquad \text{(III-27)}$$

thus

$$\tau_R^+ \approx f(y^+) \qquad \text{(III-28)}$$

Also, by definition,

$$\nu_T \frac{dv}{dy} = \overline{v_r' v_z'} \qquad \text{(III-29)}$$

therefore

$$\frac{\nu_T}{\nu} = \frac{\tau_R^+}{\frac{dv^+}{dy^+}} \qquad \text{(III-30)}$$

Substituting (25) and (26) into (30) yields,

$$\frac{\nu_T}{\nu} = \frac{f(y^+)}{1-f(y^+)} \qquad \text{(III-31)}$$

and

$$\frac{\nu_T}{v_* r_w} = \frac{1}{R_*} \frac{f(y^+)}{1-f(y^+)} \qquad \text{(III-32)}$$

Defining the effective viscosity ν_e,

$$\frac{\nu_e}{\nu} \equiv \frac{\nu+\nu_T}{\nu} = 1 + \frac{\nu_T}{\nu} \qquad \text{(III-33)}$$

thus,

$$\frac{\nu_e}{\nu} = \frac{f(y^+)}{1-f(y^+)} + 1 = \frac{1}{1-f(y^+)} \qquad \text{(III-34)}$$

For the function $f(y^+)$ in equation (25) we shall choose the following expression [34]

$$f(y^+) = \frac{y^{+3}}{y^{+3}+N^3} - \frac{1}{E(y^+)} \frac{y^{+5}}{y^{+5}+N^5} \qquad \text{(III-35)}$$

where

$$E(y^+) = \frac{ky^+}{1+bn} \qquad \text{(III-36)}$$

N and b are constants and k is the von Karman "universal constant." It will now be shown that this model satisfies the necessary constraints.

(1) When $y^+ << N$,

$$\lim_{y^+ \to o} f(y^+) = \frac{y^{+3}}{N^3} - \frac{1}{k}\frac{y^{+4}}{N^5} \qquad \text{(III-37)}$$

Substituting (37) into (27) yields,

$$\lim_{y^+ \to o} \frac{dv^+}{dy^+} = 1 - \frac{y^{+3}}{N^3} + \frac{1}{k}\frac{y^{+4}}{N^5} \qquad \text{(III-38)}$$

which satisfies the constraint given by (9). Integrating equation (38) from the wall to y^+ gives,

$$\lim_{y^+ \to o} v^+ = y^+ - \frac{1}{4N^3} y^{+4} + \frac{1}{5kN^5} y^{+5} \qquad \text{(III-39)}$$

which satisfies the constraint given by (8). Substitution of (37) into (28) yields,

$$\lim_{y^+ \to o} \tau_R^+ = \frac{y^{+3}}{N^3} - \frac{1}{k}\frac{y^{+4}}{N^5} \qquad \text{(III-40)}$$

which satisfies the constraint given by (11). Substitution

of (37) into (31) yields,

$$\lim_{y^+ \to o} \frac{\nu_T}{\nu} = \frac{y^{+3}}{N^3} - \frac{1}{k}\frac{y^{+4}}{N^5} \qquad \text{(III-41)}$$

which satisfies the constraint given by (10).

(2) Considering the case when $y^+ >> N$,

$$\lim_{y^+ >> N} f(y^+) = 1 - \frac{1}{E}(y^+) \qquad \text{(III-42)}$$

or

$$\lim_{y^+ >> N} f(y^+) = 1 - \frac{1+bn}{ky^+} \qquad \text{(III-43)}$$

Substitution of (43) into (26) yields

$$\lim_{y^+ >> N} \frac{dv^+}{dy^+} = \left\{\frac{1+b(y^+/R_*)}{ky^+}\right\}(1-y^+/R_*) \qquad \text{(III-44)}$$

when $y^+/R_* << 1$ this becomes

$$\frac{dv^+}{dy^+} = \frac{1}{ky^+} \qquad \text{(III-45)}$$

which satisfies the constraint required by (14). Substitution of (43) into (25) yields,

$$\lim_{y^+>>N} \tau_R^+ = [1 - \frac{1}{ky^+} - \frac{b}{kR_*}](1-n) \qquad \text{(III-46)}$$

Note that the bracketed quantity is a function of R_*, thus making τ_R^+ a function of R_* (see Figure 2). For a given value of R_* the bracketed quantity is approximately a constant less than, but close to one, in the intermediate region. This satisfies the constraint given by (15). Substitution of (42) into (31) yields,

$$\lim_{y^+>>N} \frac{\nu_T}{\nu} = E(y^+)-1 \qquad \text{(III-47)}$$

therefore in this region,

$$E(y^+) = 1 + \frac{\nu_T}{\nu} = \nu_e \qquad \text{(III-48)}$$

Substituting (36) into (47),

$$\lim_{y^+>>N} \frac{\nu_T}{\nu} = \frac{ky^+}{1+bn} - 1 \qquad \text{(III-49)}$$

when $y^+/R_* << 1$ but $ky^+ >> 1$ this becomes

$$\frac{\nu_T}{\nu} \approx ky^+ \qquad \text{(III-50)}$$

or

$$\frac{\nu_T}{v_* r_w} \approx kn \qquad \text{(III-51)}$$

which satisfies the constraint given by (16). When $y^+/R_* \to 1$, that is, in the core, equation (44) becomes

$$\frac{dv^+}{dn} \approx \left[\frac{1+bn}{kn}\right](1-n) \qquad \text{(III-52)}$$

or,

$$\frac{dv^+}{dn} \approx \left[\frac{1}{kn} + \frac{b}{k}\right](1-n) \qquad \text{(III-53)}$$

which satisfies the constraint given by (21). Substituting (42) into (32),

$$\lim_{y^+ >> N} \frac{\nu_T}{v_* r_w} = \frac{E(y^+)-1}{R_*} \qquad \text{(III-54)}$$

or

$$\lim_{y^+ >> N} \frac{\nu_T}{v_* r_w} \approx \frac{kn}{1+bn} \qquad \text{(III-55)}$$

at n = 1

$$\left.\frac{\nu_T}{v_* r_w}\right|_{n=1} = \frac{k}{1+b} \qquad \text{(III-56)}$$

which satisfies the constraint given by (23). Thus, this model satisfies all the constraints outlined in Section 3.3.

Recall that the velocity distribution is obtained by substituting the Reynolds stress model into the Reynolds equation and integrating with respect to y^+ (or n). Due to the fact that integration is an averaging process, a model that yields good agreement with the experimental data on Reynolds stresses should yield even better agreement with the velocity profile. Moreover, the friction factor, being determined from the nondimensional average velocity, is obtained by yet another integration. Thus, a satisfactory model of the velocity distribution and the friction factor, the quantities of practical importance, can be obtained from a model that gives fair agreement with the Reynolds stresses.

It is also important to note that the Reynolds stresses being due to velocity fluctuations, are a physical parameter that can be directly measured by an experiment. This is not the case for the mixing length or the eddy diffusivity, which must be calculated by first obtaining the velocity profile and then differentiating to determine the velocity gradient. This may result in significant error in the core, where the velocity profile is flat. Thus, it is advantageous to model the Reynolds stresses by a position dependent model rather than by a "gradient transport" model.

3.5 Comparison of the Model with Experimental Results

3.5.1 Reynolds Stresses

As mentioned, there are numerous experimental data on the Reynolds stresses; the most extensive experimental analysis being due to Laufer [4] and Sandborn [5].

Recall equation (25)

$$\frac{\overline{v_r' v_z'}}{v_*^2} = f(y^+)(1-n)$$

Substituting in equation (35) yields the model for the Reynolds stress,

$$\frac{\overline{v_r' v_z'}}{v_*^2} = \left[\frac{y^{+3}}{y^{+3}+N^3} - \frac{(1+b\ y^+/R_*)}{ky^+}\frac{y^{+5}}{y^{+5}+N^5}\right](1-y^+/R_*) \qquad \text{(III-57)}$$

The model is compared with experimental data throughout the entire pipe in Figure 2. Note that for high Reynolds number flow, the Reynolds stresses obtain a maximum value very near the wall and thereafter account almost entirely for the total stress. However, it is shown in Section 3.5.2 (see equation (63)) that assuming that the total stress is equal to the Reynolds stress leads to a flat velocity profile, i.e. slug flow. Since the velocity defect data show that there is indeed a velocity defect in the core, there must be a finite difference between the total stress and the Reynolds

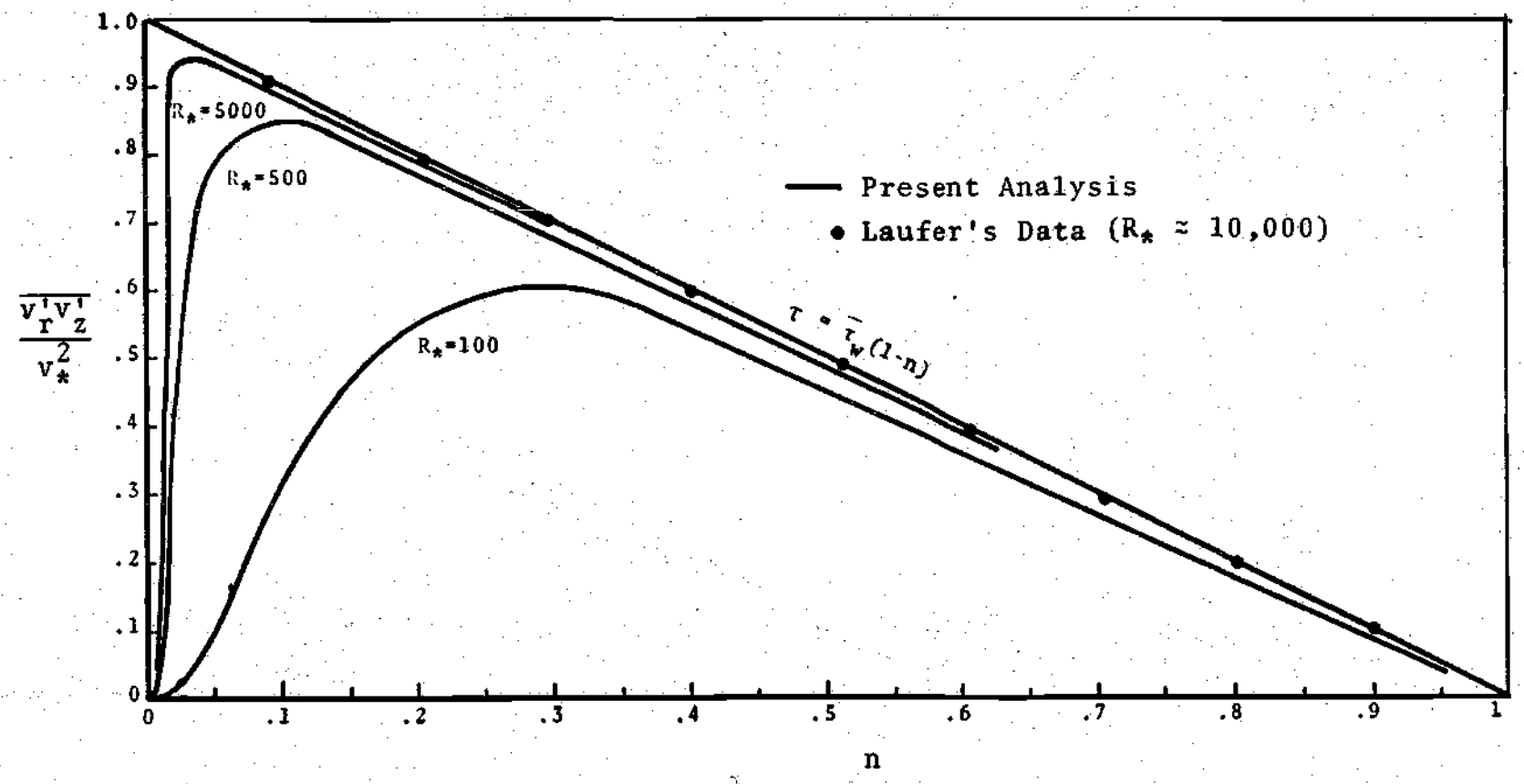

Figure 2. Comparison of the Present Analysis with Experimental Data on Reynolds Stresses for the Entire Pipe

stress, even in the core. Also note from Figure 2 that the assumption of a constant stress is only valid for a very small region of the pipe.

The comparison with experimental data in the near wall region is given in Figure 3. Because the data are very near the wall the length scale y^+ is used. Note that the Reynolds stress model approaches the wall as a third and fourth order polynominal, as given by the constraint in equation (11). Recall equation (40),

$$\lim_{y^+ \to o} \tau_R^+ = \frac{y^{+3}}{N^3} - \frac{1}{k} \frac{y^{+4}}{N^5}$$

the model approximation for the near wall region. Since k is the von Karman "universal constant," the only unknown constant is N. Thus, the experimental data on the Reynolds stresses very near the wall is used to determine the value of N.

From Figures 2 and 3 it is noted that the proposed model is in good agreement with the experimental data throughout the core as well as the near wall region. As mentioned, the velocity profile is determined by integrating of the Reynolds equation. Thus, good agreement with the Reynolds stresses should lead to an accurate prediction of the velocity distribution. It will now be shown that this is in fact the case.

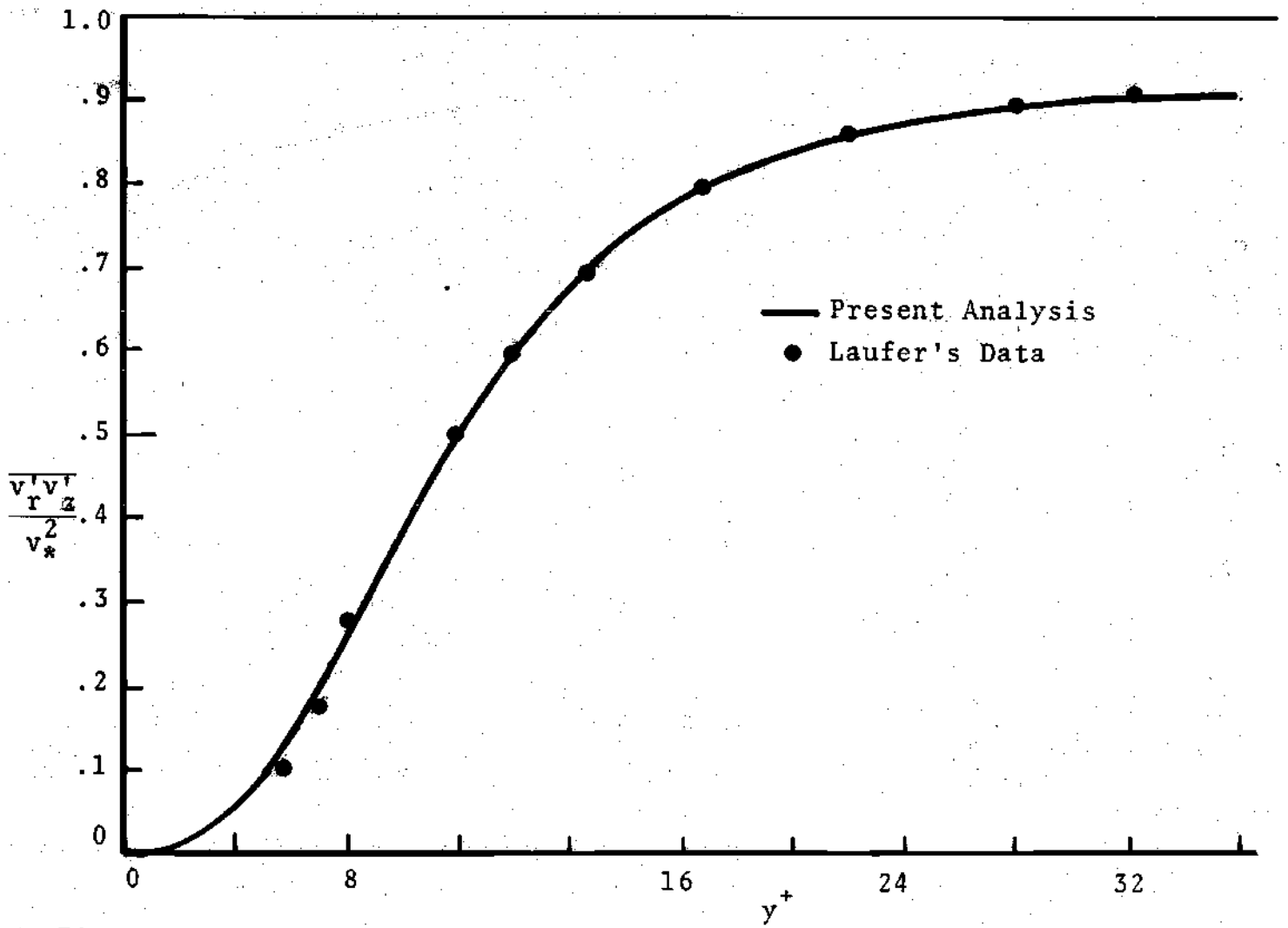

Figure 3. Comparison of the Present Analysis with Experimental Data on Reynolds Stresses Near the Wall

3.5.2 Velocity Distribution

The analytical formulation of the velocity distribution may be obtained by direct integration of the differential equation of motion as given by equations (II-24) or (II-27); the choice upon the desired dependence of the velocity on nondimensional length. Recall the Reynolds equation,

$$\frac{dv^+}{dy^+} = (1-y^+/R_*) - \frac{\overline{v_r' v_z'}}{v_*^2} \qquad \text{(III-58)}$$

or

$$\frac{1}{R_*}\frac{dv^+}{dn} = (1-n) - \frac{\overline{v_r' v_z'}}{v_*^2} \qquad \text{(III-59)}$$

Direct integration of the above equations yield,

$$v^+(y^+) = y^+[1-\tfrac{1}{2}\, y^+/R_*] - \int_0^{y^+} \frac{\overline{v_r' v_z'}}{v_*^2}\, dy^+ \qquad \text{(III-60)}$$

laminar effect turbulent effect

and,

$$v^+(n) = R_* \left\{\frac{[1-(1-n)^2]}{2} - \int_0^n \frac{\overline{v_r' v_z'}}{v_*^2}\, dn\right\} \qquad \text{(III-61)}$$

laminar effect turbulent effect

This clearly illustrates that the turbulent velocity profile must be flatter than the laminar profile, since the integrand (the Reynolds stress) is positive. The maximum velocity may be obtained immediately from equation (60) by setting $y^+ = R_*$, or from equation (61) by setting n = 1.

$$v^+(1) = R_* \{\underbrace{\frac{1}{2}}_{\text{laminar effect}} - \underbrace{\int_0^1 \frac{\overline{v'_r v'_z}}{v_*^2} dn}_{\text{turbulent effect}}\} \qquad \text{(III-62)}$$

Subtraction of equation (61) from (62) results in the "velocity defect law,"

$$v^+(1) - v^+(n) = R_* \{\frac{(1-n)^2}{2} - \int_n^1 \frac{\overline{v'_r v'_z}}{v_*^2} dn\} \qquad \text{(III-63)}$$

The velocity profile can be determined by substitution of the position dependent model of the Reynolds stress into the above expressions.

In Section 3.5.1 concerning the Reynolds stress, it was mentioned that it is often assumed that in the core the total stress is due to the Reynolds stress, that is, that $\tau_R^+ \approx (1-n)$. If this assumption is substituted into equation (63) the velocity defect becomes zero, i.e. slug flow. Moreover, the first term in equation (63) is equal to the area under the total stress "curve" from the pipe center to n, and the second term is equal to the area under the

Reynolds stress "curve" from the pipe center to n; the velocity defect is equal to the difference between these two terms, which by definition is equal to the viscous forces. The velocity defect in turbulent flow is due to the integrated effect of the viscous forces from the pipe center to n, thus the effects of viscosity, no matter how small, must be considered.

Substitution of the Reynolds stress model as given by equation (57) into equation (60) results in

$$v^+(y^+) = y^+[1-\tfrac{1}{2}y^+/R_*] - \int_0^{y^+} \left[\frac{y^{+3}}{y^{+3}+N^3} - \frac{(1+b\ y^+/R_*)}{ky^+}\ \frac{y^{+5}}{y^{+5}+N^5}\right](1-y^+/R_*)dy^+ \qquad \text{(III-64)}$$

This can be integrated to give the complete analytic expression for the velocity distribution. Doing so yields the following expression:

$$v^+(y^+) = \frac{1}{5k}\,\ell n(y^{+5}+N^5) - \frac{1}{k}\,\ell n(N)$$

$$+ \frac{N}{3}\left[\frac{1}{2}\ell n\left\{\frac{(y^++N)^3}{y^{+3}+N^3}\right\}+\sqrt{3}\left(\tan^{-1}\left\{\frac{2y^+-N}{\sqrt{3}N}\right\}-\tan^{-1}\left\{\frac{-\sqrt{3}}{3}\right\}\right)\right]$$

$$+ \frac{N^2}{3R_*}\left[-\frac{1}{2}\ell n\left\{\frac{(y^++N)^3}{y^{+3}+N^3}\right\}+\sqrt{3}\left(\tan^{-1}\left\{\frac{2y^+-N}{\sqrt{3}N}\right\}-\tan^{-1}\left\{\frac{-\sqrt{3}}{3}\right\}\right)\right]$$

$$+\frac{(b-1)}{kR_*}\left[y^+-\frac{N}{5}\left\{\ell n(y^++N)+0.309\ell n(y^{+2}+0.618y^+N+N^2)\right.\right.$$

$$-0.809\ell n(y^{+2}-1.618y^+N+N^2)+1.176\tan^{-1}\left(\frac{y^+-0.809N}{0.588N}\right)$$

$$\left.\left.+1.902\tan^{-1}\left(\frac{y^+-0.309N}{0.951N}\right)-0.512\right\}\right]$$

$$-\frac{b}{kR_*^2}\left[\frac{1}{2}y^{+2}-\frac{N^2}{5}\left\{-\ell n(y^++N)-0.309\ell n(y^{+2}+1.168y^+N+N^2)\right.\right.$$

$$+0.809\ell n(y^{+2}-1.618y^+N+N^2)+1.176\tan^{-1}\left(\frac{y^++0.309N}{0.951N}\right)$$

$$\left.\left.+1.902\tan^{-1}\left(\frac{y^+-0.809N}{0.588N}\right)-0.512\right\}\right] \qquad \text{(III-65)}$$

This expression is too complex to be of practical use, however, a much simpler expression for the velocity distribution will now be obtained. This simplified expression is in good agreement with experimental data in the viscous sublayer, through the logarithmic region and to the pipe

center. Moreover, the three velocity expressions required by the "state of the art" are seen to result from this single expression.

If in equation (64) it is assumed that $y^+/R_* << 1$ then the equation becomes,

$$v^+(y^+) = y^+ - \int_o^{y^+} \left[\frac{y^{+3}}{y^{+3}+N^3} - \frac{1}{k}\frac{y^{+4}}{y^{+5}+N^5}\right]dy^+ \qquad \text{(III-66)}$$

Integration results in the following velocity distribution:

$$v^+(y^+) = \frac{1}{5k}\ell n(y^{+5}+N^5)+\frac{\sqrt{3}}{3}N\left[\tan^{-1}\left(\frac{2y^+-N}{\sqrt{3}N}\right)+\frac{\pi}{6}\right]+\frac{N}{6}\ell n\left\{\frac{(y^++N)^3}{y^{+3}+N^3}\right\}-\frac{1}{k}\ell n(N) \qquad \text{(III-67)}$$

This expression (with N = 9.5) is plotted in Figure 4 and is seen to be in good agreement with the experimental data of Nikuradse [11] and Deissler [12] for the entire pipe. Thus, this single expression can be used to predict the velocity profile from the wall to the pipe center.

The three region approximation that is required by the "state of the art" can be shown to result from equation (67). Consider the three regions:

(1) $o \leq y^+ < 5$

Expansion of the log terms and the arctangent by Taylor series about $y^+ = o$ yields,

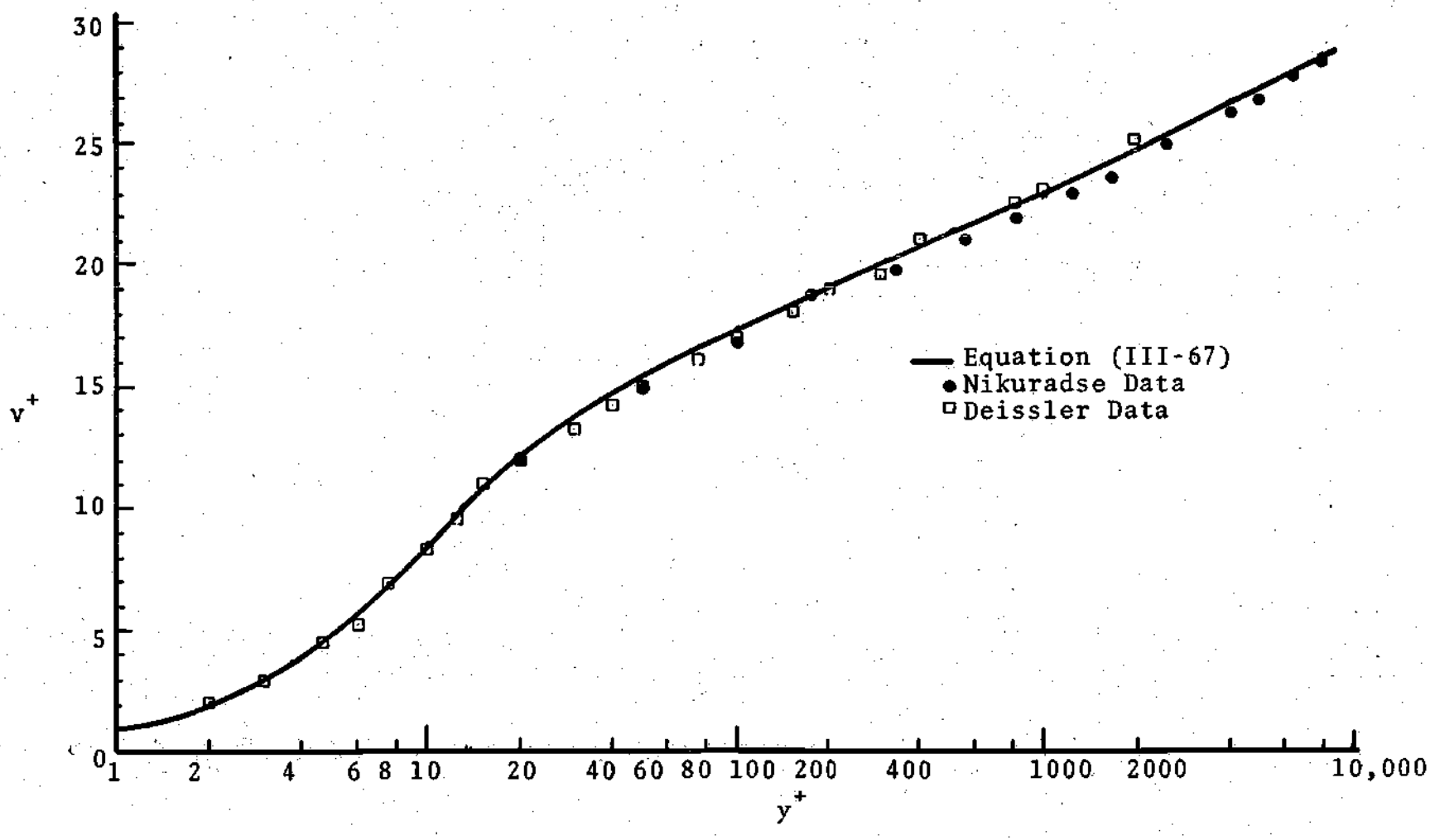

Figure 4. Comparison of the Present Analysis with Experimental Data on the Velocity Distribution for the Entire Pipe

$$v^+(y^+) = y^+ - \frac{1}{4N^3} y^{+4} + \frac{1}{5kN^5} y^{+5} \qquad \text{(III-68)}$$

For the range of y^+ considered and with N = 9.5, this expression is similar to the "state of the art" for this region as given by equation (35a).

(2) $5 < y^+ < 30$

For this region both y^+ and N are significant in the argument of the log term and thus no simple expansion can be given for equation (67). However, it is easily verified that in this region the velocity predicted by equation (67) is similar to that predicted by the "state of the art" for this region, i.e.

$$v^+(y^+) = 5\ell n(y^+) - 3 \qquad \text{(III-69)}$$

(3) $y^+ > 30$

Considering this region the following approximations are applicable,

$$\frac{1}{5k} \ell n(y^{+5}+N^5) \approx \frac{1}{5k} \ell n(y^{+5}) = \frac{1}{k} \ell n(y^+)$$

and,

$$\tan^{-1}\left(\frac{2y^+-N}{\sqrt{3}N}\right) \approx \pi/2$$

$$\ell n \left\{\frac{(y^+ + N)^3}{y^{+3} + N^3}\right\} \approx o$$

thus,

$$\frac{\sqrt{3}}{3} N\left[\tan^{-1}\left(\frac{2y^+ - N}{\sqrt{3}N}\right) + \frac{\pi}{6}\right] + \frac{N}{6} \ell n \left\{\frac{(y^+ + N)^3}{y^{+3} + N^3}\right\} \frac{-1}{k} \ell n(N) \approx 5.8$$

(with N = 9.5)

With this approximation equation (67) becomes,

$$v^+(y^+) = \frac{1}{k} \ell n(y^+) + 5.8 \qquad \text{(III-70)}$$

Thus in the appropriate region, equation (67) reduces to the "log law" obtained by Prandtl and von Karman and the constant in the "log law" is seen to result from the arctangent and the second log term approaching an asymptotic value.

In Figure 5 equation (67) is compared with experimental data for the intermediate region and in Figure 6 it is compared with experimental data for the near wall region. From these two figures and Figure 4 it is seen that the expression for the velocity distribution as given by equation (67) is in good agreement with experimental data throughout the entire pipe, that is, from the wall to the

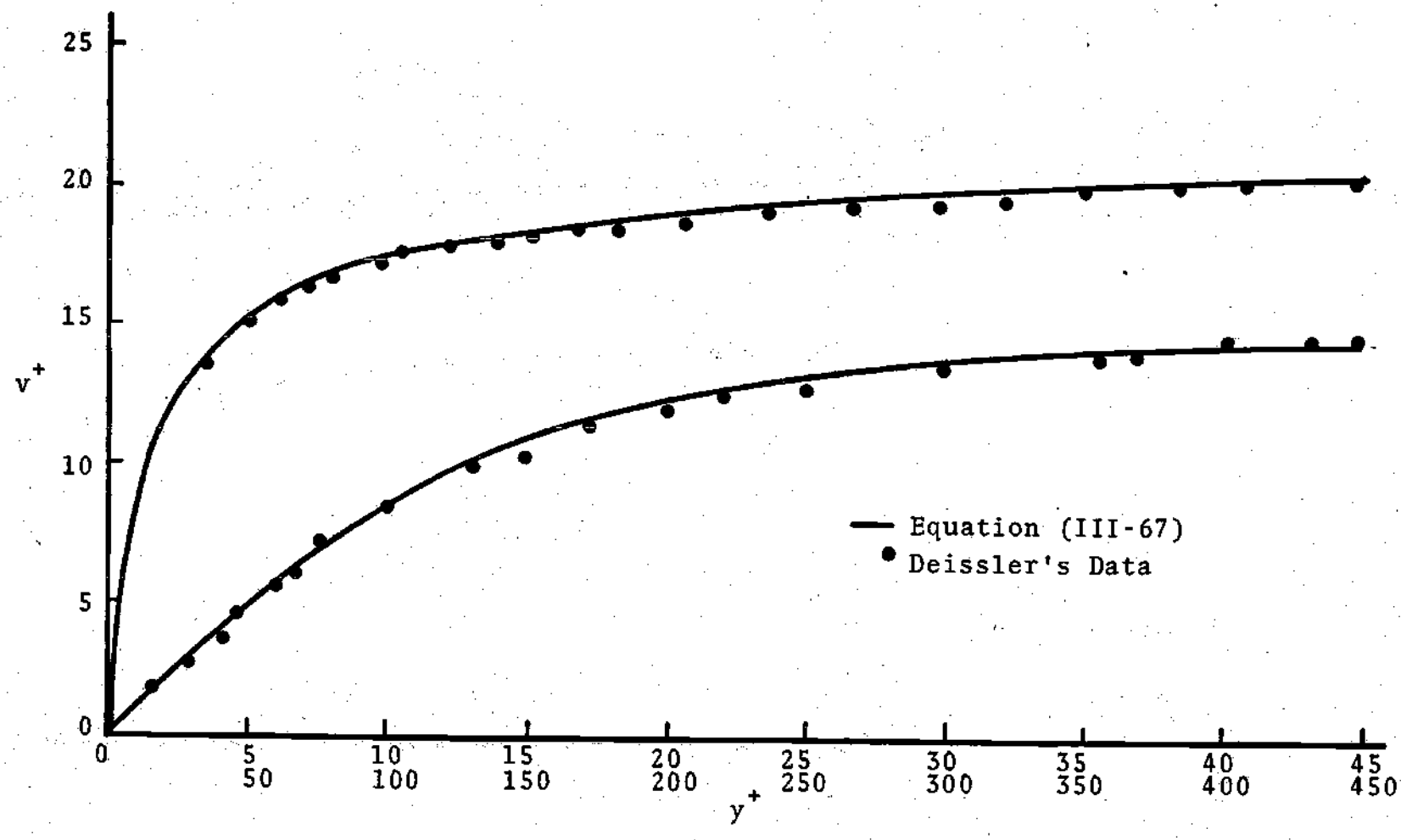

Figure 5. Comparison of the Present Analysis with Experimental Data on the Velocity Distribution for the Intermediate Region

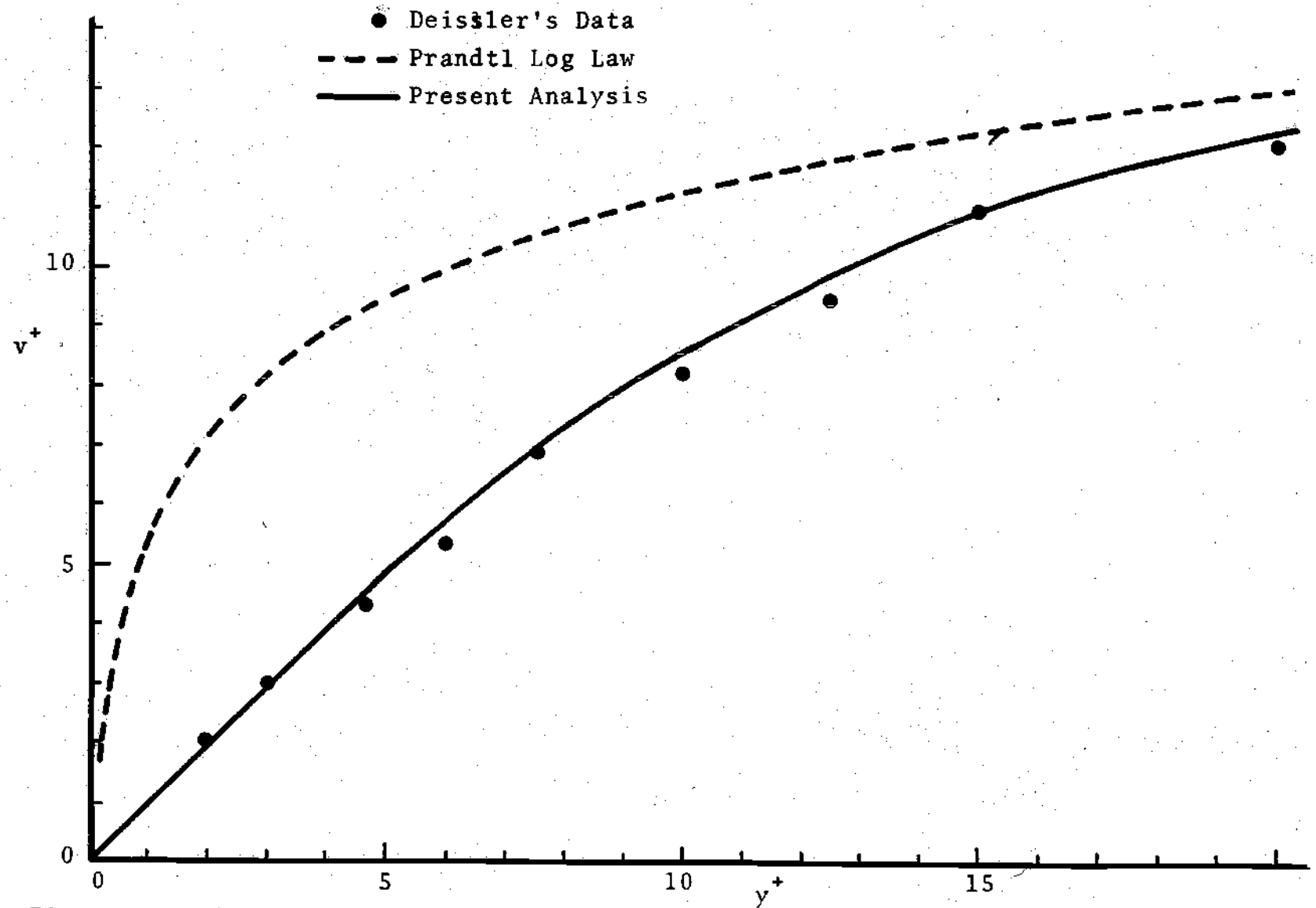

Figure 6. Comparison of the Present Analysis with the "Log Law" and Experimental Data for the Near Wall Region

pipe centerline. Thus, this single expression can replace the three expressions required by the "state of the art."

The "velocity defect law" can be obtained by substitution of the Reynolds stress model into equation (63), however, the resulting expression is formidable. Rather, due to the fact that the "velocity defect law" is used to represent flow in the core region, the approximate expression as given by equation (53) can be employed. Recall equation (53),

$$\frac{dv^+}{dn} = \left[\frac{1}{kn} + \frac{b}{k}\right] (1-n)$$

Integrating from n to 1 gives the "velocity defect law"

$$v^+(1)-v^+(n) = \frac{1}{k}\left[\ell n\left(\frac{1}{n}\right)-(1-n) + \frac{b}{2}(1-n)^2\right] \qquad \text{(III-71)}$$

This result is compared with the experimental data of Nikuradse [11], von Karman [14], and Stainton [15] in Figure 7. Fair agreement is obtained with the experimental data; the best agreement being in the core, the region in which the assumptions leading to equation (71) are most valid. It is important to realize that the velocity defect is obtained by subtracting two velocities. If some experimental error is made in measuring the velocity itself or in positioning the instrument probe, significant error is being

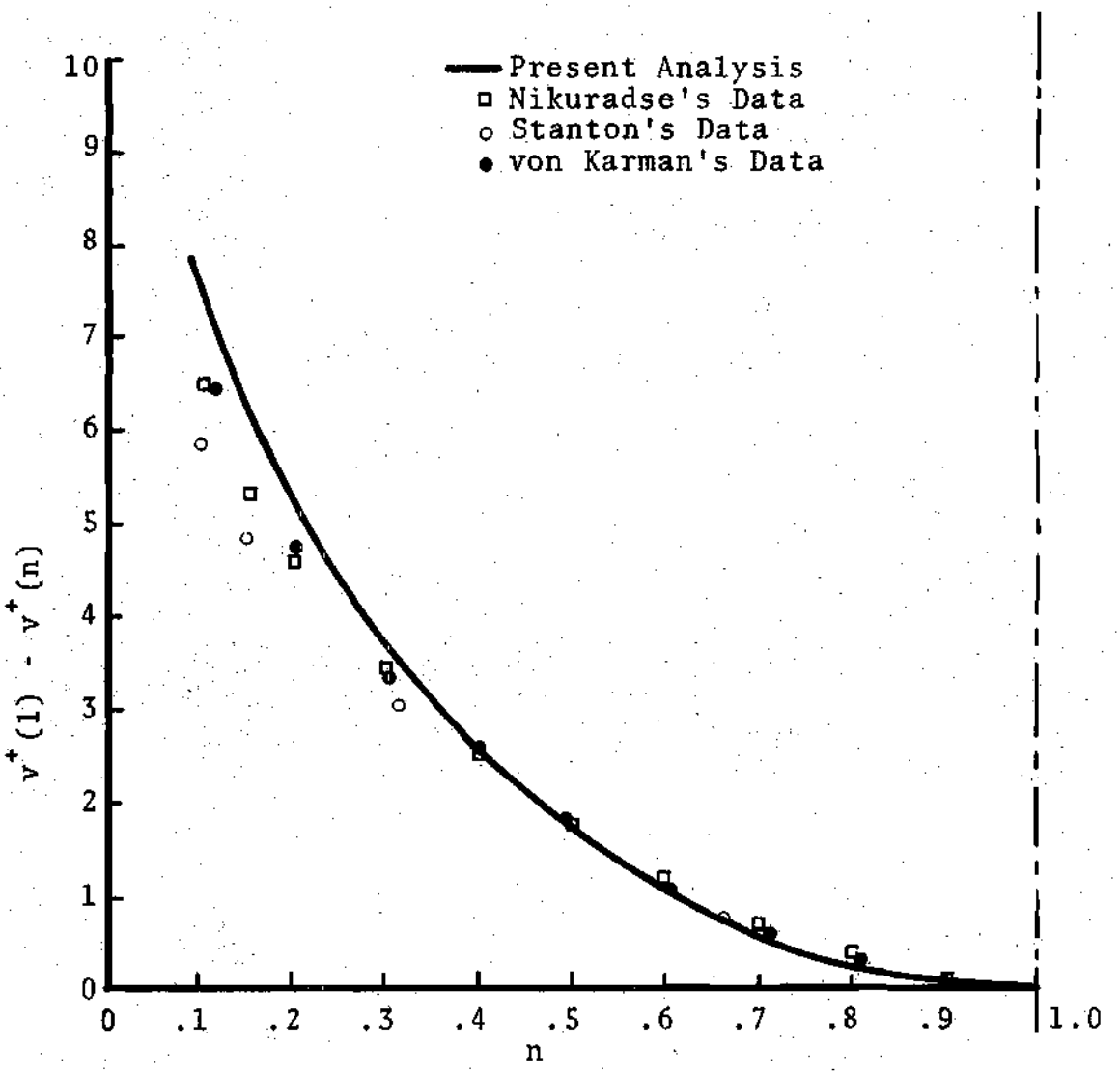

Figure 7. Comparison of the Present Analysis with Experimental Data on the "Velocity Defect Law"

introduced into the defect law "data," however, this error is of small consequence in the velocity profile (as in Figure 4). Thus, the velocity profile itself, not the defect law, should be the experimental data used to evaluate a turbulence model. The present analysis is in good agreement with the velocity profile data.

It was noted in the section entitled General Observations Concerning Turbulent Flows, that two length scales are associated with the phenomena of turbulence. One length scale pertains to the flow region near the wall where viscous forces are predominate; the other pertains to the core, where inertial forces are dominant. The model proposed by this thesis contains two constants: N and b. (This is also the case with the formulations of Prandtl and von Karman). Two constants are required since turbulence has two length scales. One of the constants, N, was determined from data pertaining to the viscous region since the other constant, b, did not appear in the approximation applicable to this region (see Section 3.5.1). The constant, b, is determined from data pertaining to the inertial region (the "velocity defect law") since the constant, N, did not appear in the approximation applicable to this region (see equation (71)); thus justifying the need and the manner of determining the two constants.

In concluding this section on the velocity distribution, it should be emphasized that the present analysis yields a

single expression for the velocity distribution that is in agreement with the experimental data from the wall to the pipe center. While the exact analytic expression is somewhat complex, a simplified expression is given and is seen to be in agreement with the velocity profile predicted by the state of the art. Moreover, the integral formulation of the velocity profile, which is valid for the entire pipe, (given by equation (64)) lends itself to computer application to the more difficult problem of turbulent convective heat transfer.

3.5.3 Average Velocity and the Friction Factor

By definition of the average velocity,

$$\langle v \rangle = \frac{1}{\pi r_w^2} \int_0^{r_w} v(r) 2\pi r dr \qquad \text{(III-72)}$$

This can be integrated by parts, thus expressing the average velocity in terms of the velocity gradient.

$$\langle v \rangle = \frac{v(r) r^2}{r_w^2} \Big|_0^{r_w} - \int_0^{r_w} \frac{\partial v}{\partial r} \left(\frac{r}{r_w}\right)^2 dr \qquad \text{(III-73)}$$

The first term is zero from the boundary conditions. Dividing by v_* and introducing the dimensionless length scales,

$$\frac{\langle v \rangle}{v_*} = \int_0^1 \frac{\partial v^+}{\partial n} (1-n)^2 dn \qquad \text{(III-74a)}$$

or

$$\frac{\langle v \rangle}{v_*} = \int_0^{R_*} \frac{\partial v^+}{\partial y^+} (1-y^+/R_*)^2 dy^+ \qquad \text{(III-74b)}$$

Substituting the expression for the velocity gradient as given by equation (26) yields

$$\frac{\langle v \rangle}{v_*} = \int_0^{R_*} \{1-f(y^+)\}(1-y^+/R_*)^3 dy^+ \qquad \text{(III-75)}$$

or in terms of the model for $f(y^+)$ as given by equation (35)

$$\frac{\langle v \rangle}{v_*} = \int_0^{R_*} \{1 - \frac{y^{+3}}{y^{+3}+N^3} + \frac{(1+b\ y^+/R_*)}{ky^+} \frac{y^{+5}}{y^{+5}+N^5}\}(1-y^+/R_*)^3 dy^+ \qquad \text{(III-76)}$$

The average velocity could be obtained by analytic integration of the above expression, however, doing so results in some sixteen terms. Rather, the above expression for the average velocity is used to obtain a more meaningful quantity, the friction factor.

By definition of the friction factor,

$$\tau_w = \frac{f}{4} \frac{\rho \langle v \rangle^2}{2} \qquad \text{(III-77)}$$

Rearranging yields

$$\frac{f}{8} = \frac{\tau_w / \rho}{\langle v \rangle^2} \qquad \text{(III-78)}$$

Recalling the definition of the friction velocity, this can be expressed as

$$\frac{f}{8} = \frac{1}{[\frac{\langle v \rangle}{v_*}]^2} \qquad \text{(III-79)}$$

or from equation (74b)

$$\frac{f}{8} = \frac{1}{[\int_0^{R_*} \frac{\partial v^+}{\partial y^+} (1 - y^+/R_*)^2 dy^+]^2} \qquad \text{(III-80)}$$

The form of this expression gives physical insight into the friction factor. The friction factor may be interpreted as the inverse square of the volume averaged rate of strain. Also note that the friction factor results from a smoothing process, that is, integration.

Substitution of the nondimensional average velocity as given by equation (76) into equation (79) yields

$$\frac{f}{8} = \frac{1}{\left[\int_0^{R_*} \left\{1 - \frac{y^{+3}}{y^{+3}+N^3} + \frac{(1+b\ y^+/R_*)}{ky^+}\ \frac{y^{+5}}{y^{+5}+N^5}\right\}(1-y^+/R_*)^3 dy^+\right]^2} \qquad \text{(III-81)}$$

This expression may be integrated to obtain an analytic expression for the friction factor. This was done, however, the result is complex. The expression for the friction factor was also numerically evaluated on a machine. The comparison of the results with values taken from the Moody chart and with the experimental data of Nikuradse [11] are given in Figure 8. It is seen that the results are in fair agreement with the accepted values of the friction factor. However, much closer agreement with the data was expected in light of the fact that the friction factor is obtained by integration of the velocity distribution, which, was shown previously to be in good agreement with many experimental data. Moreover, it is shown by Schlichting [16] that integration of the Prandtl log law (which is known to be in agreement with the velocity data of Nikuradse) also results in poor agreement with the experimental data on the friction factor. The friction factor being much easier to experimentally measure than the velocity distribution is presumably the more reliable data. Thus, in light of the above comments there is some question as to the accuracy of the experimental data on the velocity distribution.

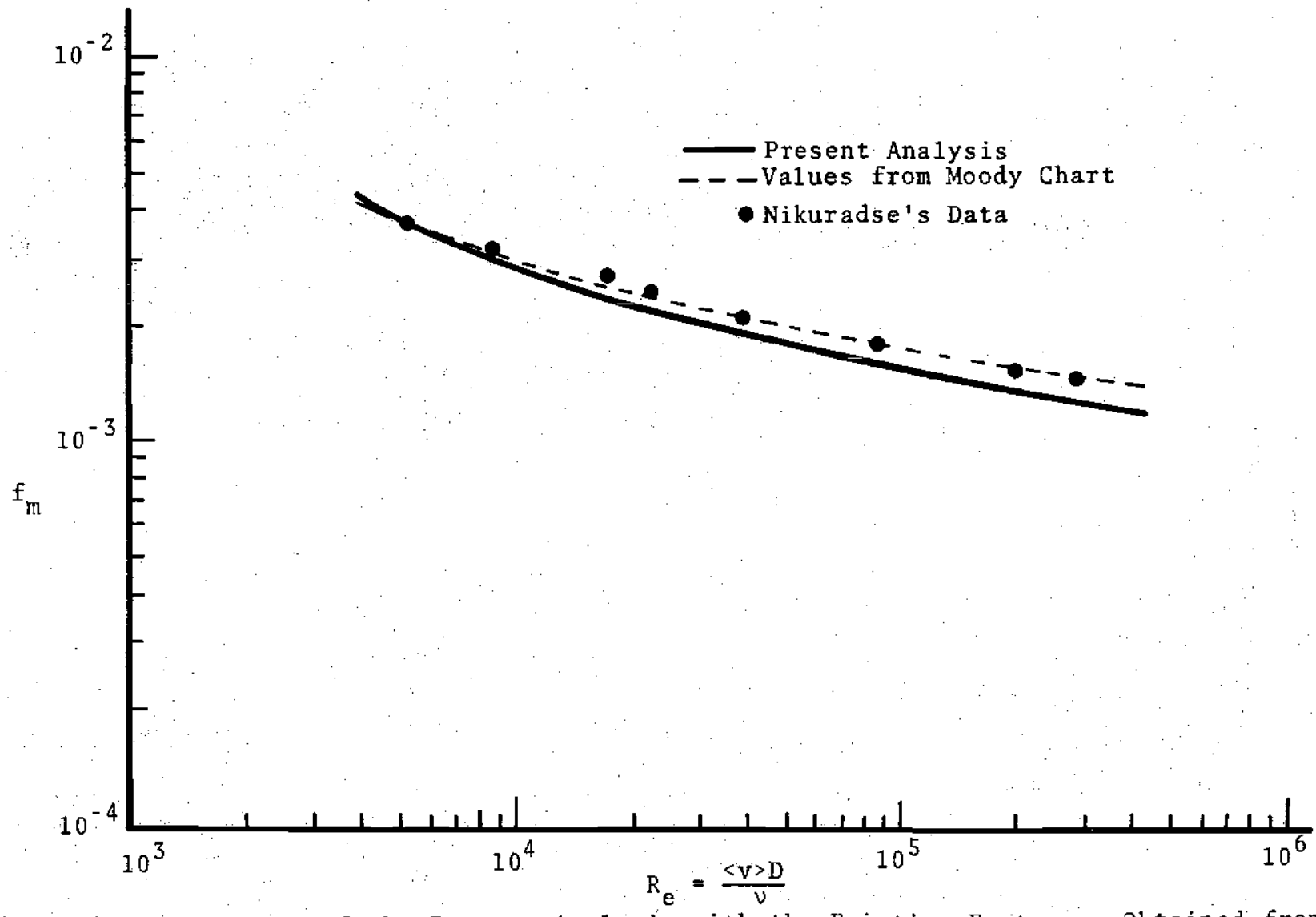

Figure 8. Comparison of the Present Analysis with the Friction Factor as Obtained from the Moody Chart and the Experimental Data of Nikuradse

3.5.4 Eddy Diffusivity

The eddy diffusivity approach is often employed as a model for convective heat transfer in turbulent flows. Because of the universal acceptance of the eddy diffusivity approach, it is important to apply the results of the present analysis to the eddy diffusivity model.

The eddy diffusivity is defined by the following equation,

$$\frac{\tau}{\rho} = (\nu+\nu_T)\frac{dv}{dy} \qquad \text{(III-82)}$$

Substitution of equation (II-5a) in the above yields,

$$\frac{\tau_w}{\rho}(1-n) = (\nu+\nu_T)\ \frac{dv}{dy} \qquad \text{(III-83)}$$

This can be expressed in dimensionless form by introducing the friction velocity and rearranging

$$(1-n) = (1 + \frac{\nu_T}{\nu})\ \frac{dv^+}{dy^+} \qquad \text{(III-84)}$$

Solving for the eddy diffusivity,

$$\frac{\nu_T}{\nu} = \frac{(1-n)}{\frac{dv^+}{dy^+}} - 1 \qquad \text{(III-85)}$$

Noting that the velocity gradient appears in the denominator of the equation defining the eddy diffusivity it is no surprise that the experimental data on the eddy diffusivity are inconsistent. Some experimental data place the maximum value of the eddy diffusivity at the pipe center while other maintain that the eddy diffusivity is zero at the centerline. (Some models even have a negative eddy diffusivity at the center.)

Substituting equation (26) into equation (85) yields,

$$\frac{\nu_T}{\nu} = \frac{f(y^+)}{1-f(y^+)} \qquad \text{(III-86)}$$

and

$$\frac{\nu_T}{v_* r_w} = \frac{1}{R_*} \frac{f(y^+)}{1-f(y^+)} \qquad \text{(III-87)}$$

Recalling the model proposed for $f(y^+)$ the above becomes,

$$\frac{\nu_T}{\nu} = \frac{\frac{y^{+3}}{y^{+3}+N^3} - \frac{(1+b\ y^+/R_*)}{ky^+} \frac{y^{+5}}{y^{+5}+N^5}}{1 - \left[\frac{y^{+3}}{y^{+3}+N^3} - \frac{(1+b\ y^+/R_*)}{ky^+} \frac{y^{+5}}{y^{+5}+N^5}\right]} \qquad \text{(III-88)}$$

This expression can be used to determine the eddy diffusivity throughout the entire pipe. However, simplified expressions for equation (86) were given in Section 3.4. Recall that for the regions:

(a) near the wall, that is, $y^+ << N$,

$$\frac{\nu_T}{\nu} = \frac{y^{+3}}{N^3} - \frac{1}{k}\frac{y^{+4}}{N^5} \qquad \text{(III-89)}$$

(b) intermediate region, $\frac{y^+}{R_*} << 1$ but $ky^+ >> 1$,

$$\frac{\nu_T}{\nu} = ky^+ \qquad \text{(III-90)}$$

or

$$\frac{\nu_T}{v_* r_w} = kn \qquad \text{(III-91)}$$

(c) in the core, $y^+ >> N$

$$\frac{\nu_T}{v_* r_w} = \frac{kn}{1+bn} \qquad \text{(III-92)}$$

The eddy diffusivity model resulting from the present analysis is compared with the experimental data close to the wall of Laufer [4] and Sleicher [17] in Figure 9. It is seen

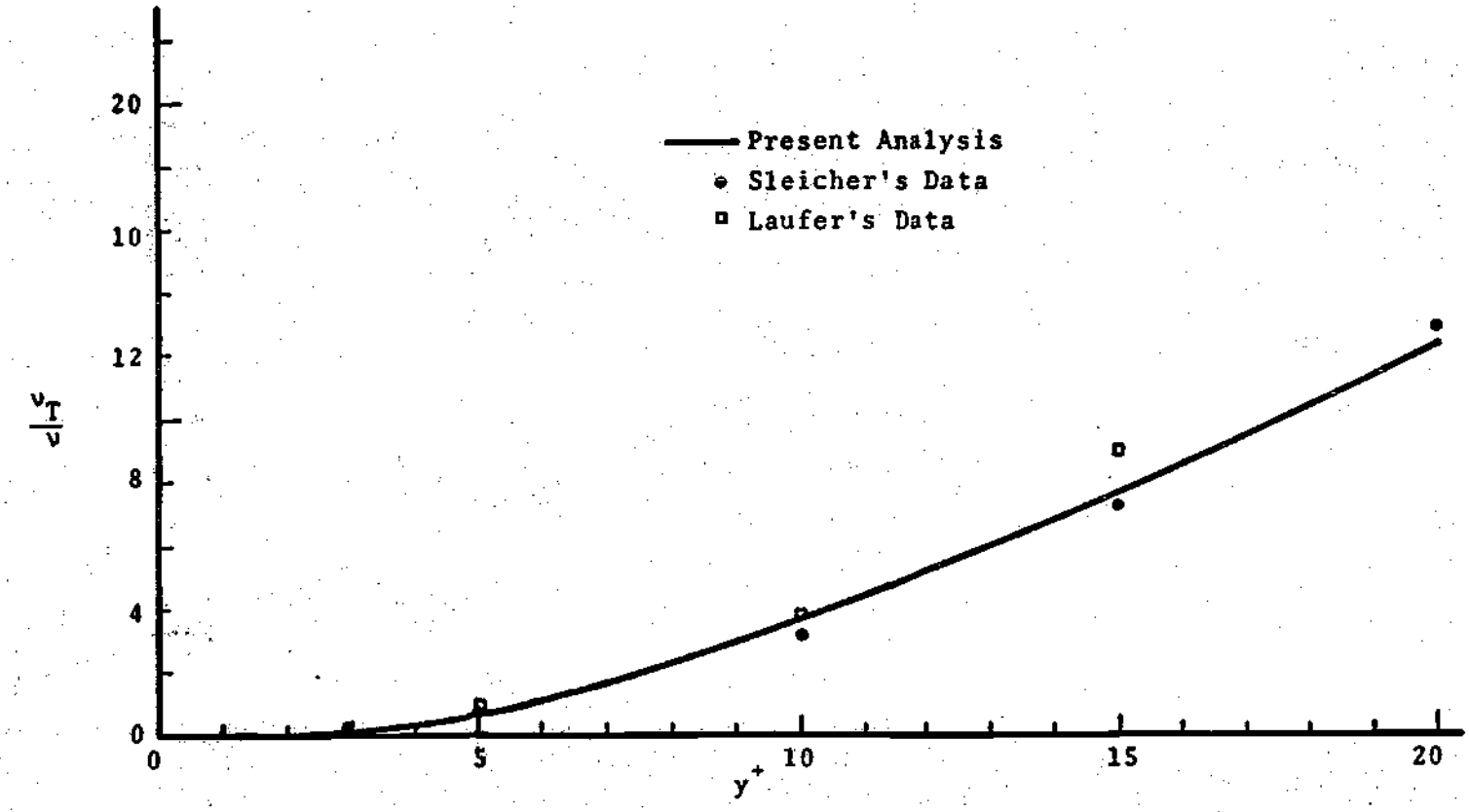

Figure 9. Comparison of the Present Analysis with Experimental Data on the Eddy Diffusivity Near the Wall

that there is good agreement in the near wall region. Also note that the turbulent viscosity is considerably larger than the mechanical viscosity for location as close to the wall as y^+ equal 20.

For the core region, the present model is compared against experimental data in Figure 10. It is noted that large scatter exists in the experimental data, as mentioned previously, this is due to the velocity gradient appearing in the denominator of the equation defining the eddy diffusivity. For the eddy diffusivity to be experimentally determined, the velocity profile must first be obtained and then differentiated to determine the velocity gradient. Significant error is possible in obtaining the derivative due to the flat velocity profile in turbulent flows. The data of Nikuradse [11] has a maximum value of the eddy diffusivity occuring at n = 0.5, and then declining to almost zero at the pipe centerline. If this result is true, then from equation (85) the velocity gradient must approach the centerline as (1-n) to the first power. There is no experimental evidence to indicate that this is in fact the case. The data of Laufer [4] and Nunner [18] indicate that the eddy diffusivity reaches a maximum value of $\frac{\nu_T}{\nu} = 0.075$ at n = 0.3 and decreases very slightly to a value of approximately 0.06 at the centerline. Gosse [19] presents experimental data to indicate that the eddy diffusivity continues to increase throughout the pipe,

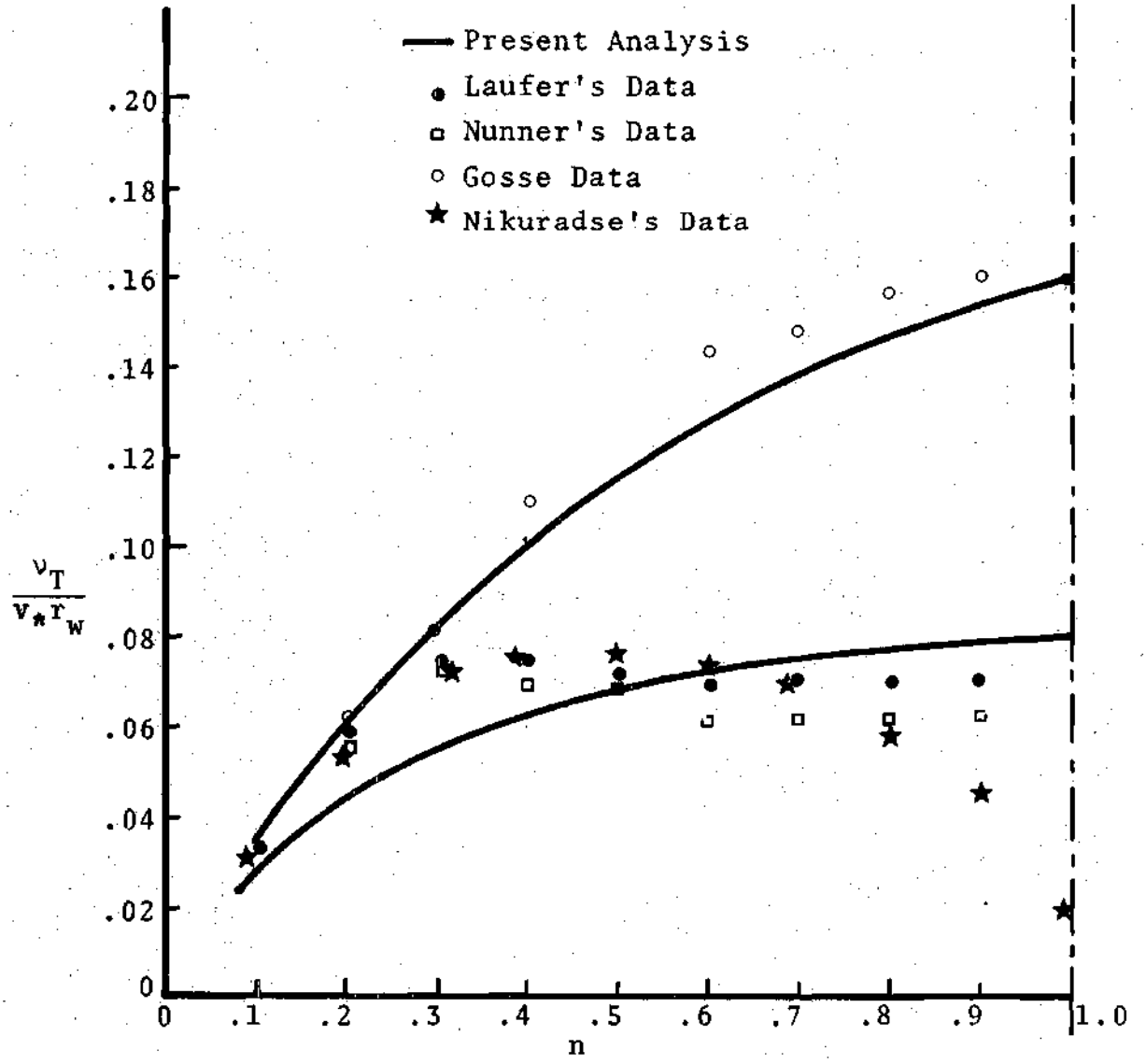

Figure 10. Comparison of the Present Analysis with Experimental Data on the Eddy Diffusivity in the Core

reaching a maximum at the centerline. This result is predicted by the present analysis which has already been shown to be in good agreement with other turbulent phenomena.

CHAPTER IV

CONCLUSIONS

The following conclusions are drawn from this work:

(1) A position dependent model of the Reynolds stresses can be formulated as an alternative to the presently employed "gradient-transport" models.

(2) The constraints placed upon any turbulence model by analytic formulation, boundary conditions, and experimental data can be satisfied with a position dependent model.

(3) The formulation can be used to accurately model turbulent phenomena, in particular:

(i) the Reynolds stresses can be predicted as a function of position throughout the entire pipe;

(ii) a single, continuous velocity distribution can be obtained with the results being applicable from the wall to the pipe center;

(iii) the friction factor can be obtained as a function of Reynolds number, thus allowing the determination of pressure losses in turbulent flows; and

(iv) the eddy diffusivity can be formulated as a function of position, thus extending the results of the present analysis to the important area of convective heat transfer in turbulent flows.

APPENDICES

APPENDIX A

REYNOLDS EQUATION

In 1895 Osborne Reynolds introduced a procedure that can be used to simplify the Navier-Stokes equations as applied to turbulent flow. Reynolds decomposed the instantaneous turbulent flow parameters into a mean value (indicated by a bar) plus a fluctuating value (indicated by a prime), i.e.

$$v_i \equiv \overline{v_i} + v_i' \tag{A-1}$$

It follows from the definition of the fluctuating quantities that the time averaged values, $\overline{v_i'}$, are equal to zero, i.e.

$$\overline{v_i'} = o \tag{A-2}$$

However, it is generally true that the squares or products of the fluctuations are not equal to zero,

$$\overline{v_i' v_j'} \neq o \tag{A-3}$$

The formal definition of the averaging process is

$$\overline{v_i} = \lim_{T\to\infty} \frac{1}{T} \int_{to}^{to+T} v_i(t)dt \qquad (A\text{-}4)$$

with this definition the following relationships may be easily verified,

$$\overline{\overline{v_i}} = \overline{v_i} \qquad (A\text{-}5a)$$

$$\overline{\overline{v_i}v_j} = \overline{v_i}\,\overline{v_j} \qquad (A\text{-}5b)$$

$$\overline{v_i+v_j} = \overline{v}_i+\overline{v}_j \qquad (A\text{-}5c)$$

$$\overline{v_iv_j} = \overline{(\overline{v_i}+v_i')(\overline{v_j}+v_j')} = \overline{v_i}\,\overline{v_j}+\overline{v_i'v_j'} \qquad (A\text{-}5d)$$

$$\overline{\frac{\partial \overline{v_j}}{\partial x_i}} = \frac{\partial \overline{v_j}}{\partial x_i} \qquad (A\text{-}5e)$$

The continuity equation for steady flow can be written as

$$\frac{\partial v_i}{\partial x_i} = o \qquad (A\text{-}6)$$

where the repeated indicies indicate summation (Einstein notation). Substituting in the decomposed velocity yields

$$\frac{\partial \overline{v_i}}{\partial x_i} + \frac{\partial v_i'}{\partial x_i} = o \qquad (A\text{-}7)$$

Taking the time average of equation (7),

$$\overline{\frac{\partial \overline{v_i}}{\partial x_i}} + \overline{\frac{\partial v_i'}{\partial x_i}} = o \qquad \text{(A-8)}$$

from (5e) and (2),

$$\overline{\frac{\partial v_i'}{\partial x_i}} = o \qquad \text{(A-9)}$$

thus,

$$\overline{\frac{\partial \overline{v_i}}{\partial x_i}} = \frac{\partial \overline{v_i}}{\partial x_i} = o \qquad \text{(A-10a)}$$

Thus the continuity equation yields the result

$$\frac{\partial v_i'}{\partial x_i} = o; \quad \frac{\partial \overline{v_i}}{\partial x_i} = o \qquad \text{(A-10b)}$$

The Navier-Stokes equations written in index notation are

$$\rho\left(\frac{\partial v_i}{\partial t} + v_j \frac{\partial v_i}{\partial x_j}\right) = -\frac{\partial p}{\partial x_i} + \mu\left(\frac{\partial^2 v_i}{\partial x_j \partial x_j}\right) \qquad \text{(A-11)}$$

Substituting in the decomposed form of instantaneous quantities yields:

$$\rho\left(\frac{\partial \overline{v_i}}{\partial t} + \frac{\partial v_i'}{\partial t} + \overline{v_j}\frac{\partial \overline{v_i}}{\partial x_j} + \overline{v_j}\frac{\partial v_i'}{\partial x_j} + v_j'\frac{\partial \overline{v_i}}{\partial x_j} + v_j'\frac{\partial v_i'}{\partial x_j}\right) =$$

$$- \frac{\partial \bar{p}}{\partial x_i} - \frac{\partial p'}{\partial x_i} + \mu\left(\frac{\partial^2 \overline{v_i}}{\partial x_j \partial x_j} + \frac{\partial^2 v_i'}{\partial x_j \partial x_j}\right) \qquad \text{(A-12)}$$

The term $v_j' \frac{\partial v_i'}{\partial x_j}$ can be transformed by noting that

$$\frac{\partial v_i' v_j'}{\partial x_j} = v_i' \frac{\partial v_j'}{\partial x_j} + v_j' \frac{\partial v_i'}{\partial x_j} \qquad \text{(A-13)}$$

The first term in equation (13) is zero by the continuity equation, thus,

$$v_j' \frac{\partial v_i'}{\partial x_j} = \frac{\partial}{\partial x_j}(v_i' v_j') \qquad \text{(A-14)}$$

The next step is to take the time average of equation (12), in doing so the terms

$$\frac{\partial \overline{v_i'}}{\partial t} \; ; \; \overline{\overline{v_j}\frac{\partial v_i'}{\partial x_j}} \; ; \; \overline{v_j'}\frac{\partial \overline{v_i}}{\partial x} \; ; \; \frac{\partial^2 \overline{v_i'}}{\partial x_j^2} \; ; \; \frac{\partial \bar{p}'}{\partial x_i}$$

must be equal to zero. Thus, the momentum equation assumes the final form,

$$\rho\left(\frac{\partial \overline{v_i}}{\partial t} + \overline{v_j}\,\frac{\partial \overline{v_i}}{\partial x_j}\right) = -\frac{\partial \overline{p}}{\partial x_i} + \mu\frac{\partial^2 \overline{v_i}}{\partial x_j^2} - \frac{\partial\left(\rho \overline{v_i' v_j'}\right)}{\partial x_j} \qquad \text{(A-15)}$$

This is referred to in the literature as the Reynolds equation. Note that this equation is identical with the laminar flow form except for the last term. The quantity $\rho\overline{v_i' v_j'}$ is termed the Reynolds stress, τ_R,

$$\tau_R \equiv \rho\overline{v_i' v_j'} \qquad \text{(A-16)}$$

Note that this quantity comes from the stress term in the original form of the Navier-Stokes equation. It is shown by Tennekes and Lumley [3] that "a stress that is generated as a momentum flux can always be written as (16), no matter what mechanism causes the momentum flux."

APPENDIX B

PRESENTLY EMPLOYED MODELS OF TURBULENCE

This appendix deals with the models that are frequently applied to turbulence, in particular, the mixing length model, eddy diffusivity model, and power approximations will be analyzed. A few comments will be made regarding statistical methods. The state of the art is also reviewed. It is intended that this discussion be more detailed than that presented in the main body of the thesis.

Mixing Length Model

This approach at modeling the turbulent stress was introduced by Prandtl in the 1920's, however, the conclusions from this work have found practically universal acceptance among workers in fluid mechanics and convective heat transfer. This is primarily due to the simplicity of the obtained logarithmic velocity distribution that is in apparent good agreement with experimental data. However, the velocity distribution obtained does not satisfy the boundary conditions of turbulent flow, that is, there is a nonzero velocity at the wall (in fact, it is indeterminate) and a gradient exists at the pipe center requiring a shear stress. The data of Nikuradse [11] are in good agreement with the Prandtl velocity expression, however, there have

been reports that cast some uncertainty on the validity of Nikuradse's data, in particular, Lindgen [20] and Ross [21].

Prandtl assumed that the turbulent stress could be modeled by

$$\tau_R = \rho \ell^2 (\frac{dv}{dy})^2 \qquad \text{(B-1)}$$

As mentioned, it is necessary to specify the turbulent stress in order to obtain closure, however, Prandtl's approach introduces a new variable, ℓ, the mixing length, which requires an additional equation. Equation (1) can be expressed in nondimensional form to give

$$\frac{\tau_R}{\tau_w} = \ell^{+2} (\frac{dv^+}{dn})^2 \qquad \text{(B-2)}$$

where $\ell^+ = \ell/r_w$. Substituting this into the Reynolds equation yields,

$$\frac{1}{R_*} \frac{dv^+}{dn} = (1-n) - \ell^{+2} (\frac{dv^+}{dy^+})^2 \qquad \text{(B-3)}$$

Rearranging,

$$(\frac{dv^+}{dy^+})^2 + \frac{1}{R_* \ell^{+2}} (\frac{dv^+}{dy^+}) - \frac{(1-n)}{\ell^+} = o \qquad \text{(B-4)}$$

Using the quadratic formula,

$$\frac{dv^+}{dy^+} = \frac{1}{2}\left[\frac{-1}{R_* \ell^{+2}} \pm \sqrt{\frac{1}{R_*^2 \ell^{+4}} + \frac{4(1-n)}{\ell^{+2}}}\right] \tag{B-5}$$

It is necessary to choose the plus sign in order that the velocity gradient be zero at the centerline. Doing so and rearranging gives,

$$\frac{dv^+}{dn} = \frac{1}{2R_* \ell^{+2}} \left\{\sqrt{1+4(1-n)R_*^2 \ell^{+2}} - 1\right\} \tag{B-6}$$

Equation (6) is an exact expression and can be used to determine the velocity profile provided there exists an equation describing the mixing length as a function of n. Equation (1) can be rearranged to give,

$$\ell = \frac{\sqrt{\tau R/\rho}}{\frac{dv}{dy}} \tag{B-7}$$

Note that equation (7) is indeterminate at the pipe centerline: one of the disadvantages to the mixing length approach.

Equation (6) can be used to clearly show the assumption necessary to arrive at the Prandtl velocity expression. For regions that are not near the wall nor the pipe core, it can be assumed that

$$4(1-n)R_*^2\ \ell^{+2} >> 1 \tag{B-8}$$

Assuming this, equation (6) gives

$$\frac{dv^+}{dn} = \frac{\sqrt{1-n}}{\ell^+} \tag{B-9}$$

In this region $n<<1$ and it is assured that $\sqrt{1-n}\approx 1$.

$$\frac{dv^+}{dn} = \frac{1}{\ell^+} \tag{B-10}$$

Prandtl assumed the mixing length to be proportional to n (see Figure 11), i.e.

$$\ell^+ = kn \tag{B-11}$$

Thus from equation (10)

$$\frac{dv^+}{dn} = \frac{1}{k}\frac{1}{n} \tag{B-12}$$

This is usually expressed in terms of y^+,

$$\frac{dv^+}{dy^+} = \frac{1}{k}\frac{1}{y^+} \tag{B-13}$$

and integration gives

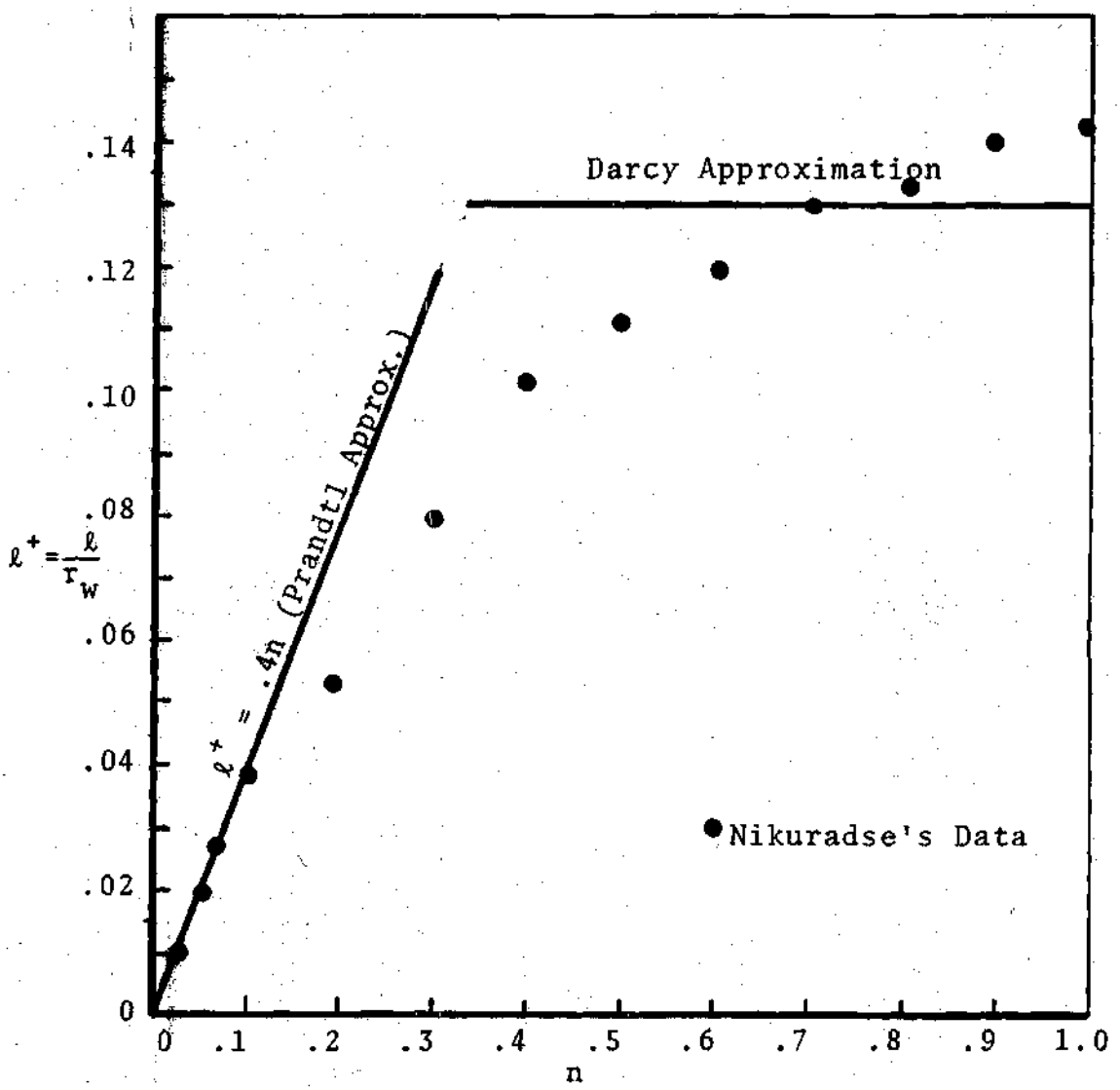

Figure 11. Mixing Length: Experimental Data and Approximations

$$v^+(y^+) = \frac{1}{k} \ln(y^+) + \text{constant} \qquad \text{(B-14)}$$

This is the Prandtl velocity distribution or the so-called "log law." k is the von Karman "universal constant" equal to 0.4 and the constant is usually chosen to be 5.5. Due to the assumption involved in equation (8) the log law should not be valid at the pipe center, nevertheless, equation (12) integrated to the pipe center gives the "velocity defect law"

$$v^+(1)-v^+(n) = \frac{1}{k} \ln(1/n) \qquad \text{(B-15)}$$

This expression should fit the data as a straight line if plotted on semi-log paper. Figure 12 shows that there is good agreement only in a limited region of the pipe.

Prandtl assumed the mixing length to be proportional to n. From Figure 11 it is seen that the mixing length could be assumed constant. This is a particularly good approximation in the core. Assuming $\ell^+ = 0.13$ results in a model obtained by H. Darcy [22] in 1855. From equation (9) it is seen that a constant mixing length results in

$$v^+(1)-v^+(n) = \text{constant} \times (1-n)^{3/2} \qquad \text{(B-16)}$$

If the constant is taken as 5.08, this expression is in better agreement with the experimental data for the core region ($n > .25$) than is the logarithmic defect law.

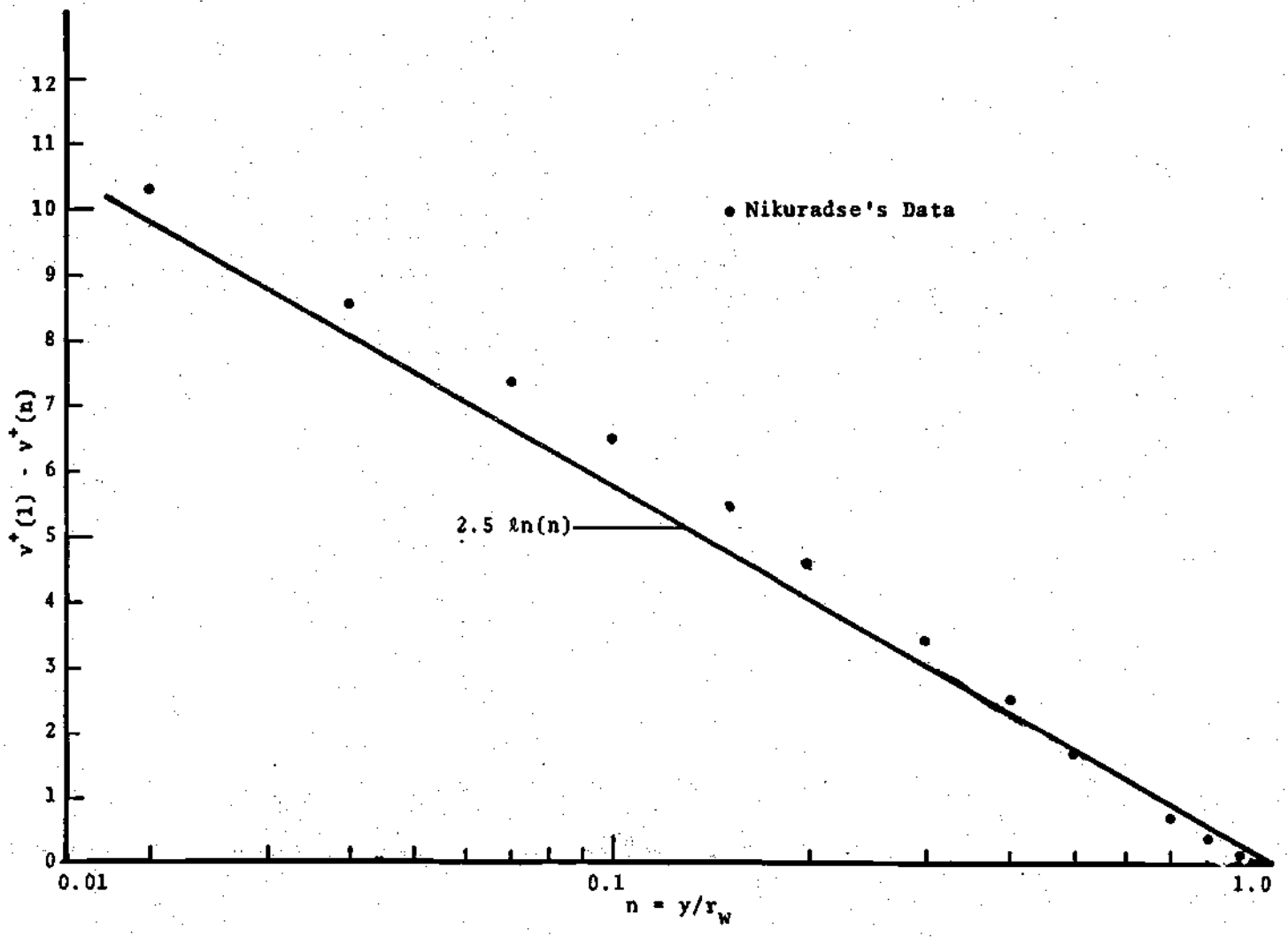

Figure 12. Velocity Defect Data on Semi-Log Coordinates

For the region near the pipe center 1-n≈o and near the wall, $\ell^+ \approx kn \approx o$, thus it can be assumed that

$$4(1-n)R_*^2\ell^{+2} << 1 \qquad \text{(B-17)}$$

With this assumption, equation (6) is of the form

$$F(x) = \sqrt{1+x} \qquad \text{(B-18)}$$

with $x << 1$

Thus, $F(x) \approx 1 - x/2$

Therefore,

$$\frac{dv^+}{dn} = R_*(1-n) \qquad \text{(B-19)}$$

Integrating this near the pipe center gives

$$v^+(1) - v^+(n) = \frac{R_*}{2}(1-n)^2 \qquad \text{(B-20)}$$

Thus, according to this model the defect law should be parabolic near the pipe centerline.

Near the wall, 1-n ≈ 1 and equation (19) becomes

$$\frac{dv^+}{dn} = R_* \qquad \text{(B-21)}$$

or

$$\frac{dv^+}{dy^+} = 1 \qquad \text{(B-22)}$$

thus

$$v^+ = y^+ \qquad \text{(B-23)}$$

This expression has been shown valid for $y^+<5$.

In order to apply the mixing length model it is necessary to specify ℓ. As noted above, Prandtl assumed ℓ^+ proportional to the relative distance from the wall while Darcy's formula results from the assumption of a constant mixing length. Nikuradse used his experimental data and determined ℓ from equation (7) and gave the following equation for determining ℓ^+,

$$\ell^+ = 0.14 - 0.08(1-n)^2 - 0.06(1-n)^4 \qquad \text{(B-24)}$$

Near the wall this can be approximated as

$$\ell^+ = 0.4n - 0.44n^2 \qquad \text{(B-25)}$$

The Russian, Kutateladze [23], suggested

$$\ell^+ = 0.39n - 0.36n^2 + 0.11n^3 \qquad \text{(B-26)}$$

In conclusion it should be emphasized that the mixing length approach has some deficiencies. Recalling equation (7)

$$\ell = \frac{\sqrt{\tau_{R/\rho}}}{\frac{dv}{dy}} \qquad \text{(B-27)}$$

note that near the pipe center $\tau_R^+ \simeq 1\text{-}n$ and employing equation (19),

$$\ell \approx \frac{\sqrt{1-n}}{1-n} = \frac{1}{\sqrt{1-n}} \qquad \text{(B-28)}$$

Thus, the mixing length is indeterminate at the pipe center Moreover, some authors, Tennekes and Lumley [4], state that "a gradient-transport model which links stress to the rate of strain at the same point in space and time cannot be used for turbulent flow."

Eddy Diffusivity Model

The concept of eddy diffusivity was first introduced by J. Bossinesq [2] in 1877. Eddy diffusivity is a logical first extension of the laminar viscosity concept in that it assumes the existence of a turbulent viscosity coefficient relating the turbulent shear stress directly to the velocity

gradient. That is,

$$\tau = - (\mu+\mu_T) \frac{d\bar{v}}{dr} \qquad \text{(B-29)}$$

This would be a simple model provided there existed a unique turbulent viscosity coefficient for each fluid, however, this is not the case. Experiments show that μ_T is a function of the fluid flow in addition to the fluid itself. Moreover, for a given fluid flow, μ_T varies across the pipe, i.e. it is a function of the relative distance from the wall. Thus an additional equation is needed to specify the eddy diffusivity in order to obtain closure.

Equation (29) can be rearranged to give

$$\frac{\tau}{\rho} = -(\nu+\nu_T)\frac{d\bar{v}}{dr} \qquad \text{(B-30)}$$

or since the total stress is linearly related to the wall shear stress,

$$\frac{\tau_w}{\rho}(1-n) = -(\nu+\nu_T)\frac{d\bar{v}}{dr} \qquad \text{(B-31)}$$

Introducing the friction velocity, this can be expressed in dimensionless form as

$$\frac{dv^+}{dn} = R_* \frac{(1-n)}{1+\frac{\nu_T}{\nu}} \tag{B-32}$$

thus

$$v^+(n) = R_* \int_0^n \frac{(1-n)dn}{1+\frac{\nu_T}{\nu}} \tag{B-33}$$

If $\frac{\nu_T}{\nu} << 1$ then the laminar profile results, i.e.

$$v^+(1) - v^+(n) = \frac{R_*}{2} (1-n)^2 \tag{B-34}$$

If $\frac{\nu_T}{\nu} >> 1$ and assumed constant then

$$v^+(1) - v^+(n) = \frac{\nu}{\nu_T} R_* (1-n)^2 \tag{B-35}$$

This result is similar to the expression obtained by Darcy for the velocity defect in the core. Thus, specifying $\frac{\nu_T}{\nu}$ as a function of n immediately determines the velocity distribution. Several investigations, Deissler [24], van Dreist [25], and von Karman [26] have attempted to obtain this relationship. Deissler suggested the following equation for flow near a boundary,

$$\frac{\nu_T}{\nu} = a^2 v^+ y^+ [1-\exp(-a^2 v^+ y^+)] \tag{B-36}$$

where "a" must be experimentally determined. This can be expanded near the wall by recalling that $v^+ = y^+$ near the wall and expanding the exponential to yield

$$\frac{\nu_T}{\nu} \sim y^{+4} \tag{B-37}$$

It has been shown by Davies [27] that near the wall

$$\frac{\nu_T}{\nu} = c_3 y^{+3} - c_4 y^{+4} \tag{B-38}$$

thus the expression suggested by Deissler (and also van Diest) does not approach the wall correctly. Theodore von Karman assumed that turbulent fluctuations are similar at all points in the flow field (similarity hypothesis); and concluded that

$$\nu_T = k^2 \frac{(\frac{dv}{dy})^3}{(\frac{d^2v}{dy^2})^2} \tag{B-39}$$

when k is the von Karman universal constant equal to 0.4. The use of von Karman's expression gives a logarithmic defect law that differs only slightly from Prandtl's. Equation (33) can be used to give the average velocity and then to express a relationship involving the friction factor,

$$\frac{1}{f}\frac{64}{R_e} = 4\int_o^1 \frac{(1-n)^3 dn}{1+\frac{\nu_T}{\nu}} \qquad \text{(B-40)}$$

The integral is a measure of the deviation from a laminar flow resistance in that for laminar flow the right-hand side be unity. This expression could be used to correlate experimental data and to give some insight into the turbulent viscosity concept. Since the eddy diffusivity model is also used in convective heat transfer it is desirable to have an acceptable model for the eddy diffusivity.

Power Approximations

A simplified approach that is often used to model turbulent flows is to assume that the nondimensional velocity is directly proportional to the nondimensional distance raised to some exponent, that is

$$\frac{v}{v_*} = c(n)(y^+)^n \qquad \text{(B-41)}$$

This approach is seen to be deficient when one considers the variation on c(n) and n required to fit experimental data; for $R_e \approx 10^3$, $n = \frac{1}{6}$, for $R_e \approx 10^5$ $n = \frac{1}{7}$ and at $R_e \approx 10^6$ $n = \frac{1}{10}$. Thus it simply is not possible to obtain a universal velocity expression by an assumed power approximation. Nevertheless, the power approximation offers some insights in that it can be shown that the relationship between the

average velocity and the maximum velocity is

$$\frac{\bar{v}}{v_{max}} = \frac{2}{(n+1)(n+2)} \tag{B-42}$$

This illustrates the fact that the turbulent velocity profile is much flatter than the laminar one. The ratio of average to maximum velocities vary from 0.79 with $n = \frac{1}{6}$ to 0.86 with $n = \frac{1}{10}$ as compared to 0.50 for a laminar profile.

With the power approximation for the velocity distribution, it can be shown that if the friction factor is assumed proportional to the Reynolds number to some exponent then this exponent must necessarily be related to the exponent in the velocity distribution. That is, if

$$f = \frac{\text{constant}}{Re^m} \tag{B-43}$$

then

$$m = \frac{2n}{n+1} \tag{B-44}$$

A commonly used expression for the friction factor is the Blausis formula,

$$f = 0.316/Re^{0.25} \tag{B-45}$$

If this is to hold then from (44) n = 7 and

$$v^+(y^+) = \text{constant} \times (y^+)^{1/7} \qquad \text{(B-46)}$$

A constant of 8.74 best fits the experimental data.

In conclusion, this simple approach gives a quantitative description of turbulent flows. Indeed, this approach is more efficient than the mixing length model in that one obtains about equal agreement with the data for less work input. Moreover, this approach has some esthetic appeal in clearly showing the intimate connection between the velocity distribution and the friction factor.

Statistical Methods

There is presently available numerous accounts of statistical turbulent models, in particular, Hinze [7], Batchelor [28], and Tennekes and Lumley [4]. This section is included for completeness rather then as an attempt to discuss the many approaches that have been taken to statistically model turbulence. It is sufficient to say that in the methods previously discussed only average values of fluctuating quantities were considered where as the statistical approach examines the distribution of fluctuation about the average value and the correlation of adjacent fluctuations. This requires the introduction of mathematical techniques such as the Fourier transform,

correlation function and probability densities. In resorting to this approach the physical insight into the problem is diminished somewhat. Moreover, the proponents of statistical applications to fluid mechanics do not enjoy the success found by the quantum physicist.

State of the Art

In order to accurately predict the velocity distribution in turbulent flow, workers in fluid mechanics divide the flow into three hydrodynamic regions with a separate velocity expression for each region. These velocity expressions are

$$v^+ = y^+ \qquad y^+<5 \qquad \text{(B-47)}$$

$$v^+ = 5\ \ell n(y^+) - 3.05 \qquad 5<y^+<30 \qquad \text{(B-48)}$$

$$v^+ = 2.5\ \ell n(y^+) + 5.5 \qquad y^+>30 \qquad \text{(B-49)}$$

Thus, for $y^+>30$ it is common practice to use the log law derived by Prandtl and von Karman. This expression appears to be in fair agreement with experimental data, however, it is easily verified that the "log law" gives a finite velocity gradient at the pipe centerline, which is certainly incorrect. Moreover, the logarithmic formulation assumes a constant shear stress across the pipe, thus it is little surprise that the "log law" does not fit the experimental data near the pipe center. There is a more fundamental

error in equations (47), (48), and (49) in that the velocity profiles are independent of Reynolds number, while there is experimental data to indicate that the velocity profile is indeed a function of the Reynolds number. The most notable account of this is due to J. O. Hinze [13], who states that "Reynolds number similarity and the consistency of the von Karman constant appear not to hold strictly." Hinze's account of many different experimental data clearly exhibits the dependency of the velocity profile on Reynolds number. In addition to the purely fluid mechanics problems, the application of three velocity expressions to forced convection heat transfer is cumbersome.

REFERENCES

1. Prandtl, L., "Uber die ausgebildete Turbulenz," Zamm 5, pp. 126-139 (1925) and Proc. 2nd Intern. Cong. Appl. Mech., Zurich (1926).

2. Boussinesq, J., "Theorie de e'ecoulement tourbillant," Mem. Pres. Acad. Sci. XXIII, 46, Paris (1877).

3. Tennekes, H. and Lumley, J., A First Course in Turbulence, The M.I.T. Press, (1972).

4. Laufer, J., "The Structure of Turbulence in Fully Developed Pipe Flow," NACA TR1174 (1954).

5. Sandborn, V. A., "Experimental Evaluation of Momentum Terms in Turbulent Pipe Flow," NACA TN3266 (1955).

6. Murphree, E. V., "Relation Between Heat Transfer and Fluid Friction," *Ind. Eng. Chem.* 24, No. 7, pp. 726-736, (1932).

7. Hinze, J. O., Turbulence, McGraw-Hill, (1959).

8. Townsend, A. A., "The Structure of Turbulent Shear Flow," Cambridge University Press (1956).

9. Monin, A. S. and Yaglom, A. M., Statistical Fluid Mechanics: Mechanics of Turbulence, Translation edited by J. Lumley, M.I.T. Press (1971).

10. Tien, C. L. and Wasan, D. T., "Law of the Wall, In Turbulent Channel Flows," *Physics of Fluids* 6, No. 1, pp. 144-145 (1963).

11. Nikuradse, J., "Gesetzmassigreitn der Turbulenten Stromung in Glatten Rohren," Forschungshet VDI 356 (1932).

12. Deissler, R., "Analysis of Turbulent Heat Transfer, Mass Transfer, and Friction in Smooth Tubes at High Prandtl and Schmidt Numbers," Lewis Flight Propulsion Lab Report 1210. "Analytical and Experimental Investigation of Adiabatic Turbulent Flow in Smooth Tubes," Lewis Flight Propulsion Lab, TN 2138 (1950).

13. Hinze, J. O., "Turbulent Pipe Flow."

14. von Karman, Th., "Mechanische Ahnlichkeit und Turbulenz," Proc. 3rd Intern. Congress Appl. Mech. Stockholm, Pt. I, 85 (1930).

15. Stanton, T. E., "The Mechanical Viscosity of Fluids," Proceedings of the Royal Society of London, 85A, 366 (1911).

16. Schlichting, H., Boundary-Layer Theory, McGraw-Hill, New York (1968).

17. Sleicher, C. A., *Transactions ASME 80*, pg. 693, (1958).

18. Nunner, W., VDI-Forschukgseft No. 455 (1956).

19. Gosse, J., "Sur l'ecoulement turbulent des fluides," Academie des Sciences, 3 Juillet (1961).

20. Lingden, E. R., "Experimental Studies on Turbulent Pipe Flows of Distilled Water," Dept. Civil Engineering, Oklahoma State University, Rept. 1AD621071 (1965).

21. Ross, D., "A New Analysis of Nikuradse's Experiments on Turbulent Flows in Smooth Pipes," Ordnance Research Lab Penn. State College, Project NR-067-139.

22. Darcy, H., "Recherches experimentales relatives aux mouvements de e'cau dans tuyaux," Mech. Pres. A'l'Academe des Sciences de e'Institut de France 15, 141 (1858).

23. Kutateladze, S. S., Turbulent Boundary Layers in Compressible Gases, Translated by D. B. Spalding, Academic Press, New York (1964).

24. Deissler, R. G., "Investigation of Turbulent Flows and Heat Transfer in Smooth Tubes, Including the Effects of Variable Fluid Properties," *Trans. ASME 73*, No. 1, pp. 101-107 (1951). "Heat Transfer and Fluid Friction for Fully Developed Turbulent Flow of Air and Supercritical Water with Variable Fluid Properties," *Trans. ASME 76*, N-. 1, pp. 73-86 (1954).

25. van Driest, E. R., "On Turbulent Flows Near a Wall," *J. Aero. Sci. 23*, No. 11, pp. 1007-1011 (1956).

26. von Karman, Th., "The Analogy Between Fluid Friction and Heat Transfer," *Trans. ASME 61*, No. 8, November, pp. 705-710 (1939)

27. Davies, J. T., Turbulence Phenomena, Academic Press, New York (1972).

28. Batchelor, G. K., An Introduction to Fluid Mechanics, Cambridge University Press, London.

29. Kays, W. M., Convective Heat and Mass Transfer, McGraw-Hill, New York, (1966).

30. Millionshchikov, M. D., "Turbulent Flows in Boundary Layers and in Tubes," *Atomnaya Energy 28*, No. 3, pp. 207-220, (1920).

31. Brodkey, R. S., The Phenomena of Fluid Motion, Addison-Wesley, Reading, Mass., (1967).

32. Gradshteyn, I. S. and Ryzhiic, I. M., Table of Integrals, Series and Products, Translated by A. Jeffery, Academic Press, New York, (1965).

33. Reichart, H., "Vollstandige Darstelling der turbulenten Geschwindigkeitsueiteilung in glutten Leitunyen," Z. Angen. Math. Mech. 31, pp. 208-219 (1951).

34. Zuber, N., private communications.